# Cooperative Electrostatic Polymer-Antibiotic Nanoplexes

Timothy Patrick Vadala

Thesis submitted to the faculty of the Virginia Polytechnic Institute and State University
in partial fulfillment of the requirements for the degree of

Master of Science

In

Macromolecular Science and Engineering

Judy S. Riffle
Richard Turner
Richey M. Davis

May 24, 2010
Blacksburg, VA

Keywords: polyether, atom transfer radical polymerization, ATRP, core-shell, bacteria, brucella

# Cooperative Electrostatic Polymer-Antibiotic Nanoplexes

Tim Vadala

**Abstract**

Many pathogenic bacteria can enter phagocytic cells and replicate in them, and these intracellular bacteria are difficult to treat because the recommended antibiotics do not transport into the cells efficiently. Examples include food-borne bacteria such as *Salmonella* and *Listeria* as well as more toxic bacteria such as *Brucella* and the *Mycobacteria* that lead to tuberculosis. Current treatments utilize aminoglycoside antibiotics that are polar and positively charged and such drugs do not enter the cells in sufficient concentrations to eradicate the intracellular infections. We have developed core-shell polymeric drug delivery vehicles containing gentamicin to potentially overcome this challenge. Pentablock and diblock copolymers comprised of amphiphilic nonionic polyether blocks and anionic poly(sodium acrylate) blocks have been complexed with the cationic aminoglycoside gentamicin. The electrostatic interaction between the anionic polyacrylates and the cationic aminoglycosides form the cores of the nanoplexes, while the amphiphilic nature of the polyethers stabilize their dispersion in physiological media. The amphiphilic nature of the polyethers in the outer shell aid in interaction of the nanoplexes with extra- and intra-cellular components and help to protect the electrostatic core from any physiological media. This thesis investigates the electrostatic cooperativity between the anionic polyacrylates and cationic aminoglycosides and evaluates the release rates of gentamicin as a function of pH.

**Acknowledgements**

To my friends, Mike, Brian, and MJ. For all the times that I enlighten and broadened your polymer chemistry horizons. Remember this quote, "Excuse me ma'am, your daughter will be fine, I'm a polymer chemist."

To my undergraduate, Lindsay Johnson. Thank you for the opportunity for me to mentor you through the last leg of my research. There were a lot of ups and downs, but that is chemistry and science. You have been a pleasure to work with and good luck in the future and with your future endeavors.

To my brother-in-law Jeff. Thank you for being a part of my family. I especially thank you for all those hard times and long nights you spent tutoring me in physics just so I could drop the class one week before the final. Honestly, I still don't understand the subject. But hey, I got the B+ eventually. Thank you so much. Love you.

To my sister Nicole. Thank you for being such an amazing sister. You have taught me so much and continue to do so. Being the oldest isn't always the easiest, but you have done such a great job. Thank you for listening to me over the years when I needed help. Love you.

To my sister Lindsay. Thank you for being such a loving sister. You're my second Mom. You and I were blessed with experiencing college at the same time. Good times sister, good times. I thank you especially over this past year, as you were one of the underlying voices in my head telling me to not give up. Many a nights I called you to talk about problems and you always listened with no complaints. You have honestly taught me to be a better person. I might be a man in training, but soon enough I will be a man! Love you Lindsay.

To my brother Michael. Where to begin. You have truly been my mentor over the years. Without you, none of my chemistry accomplishments could have been possible. It all started 6 years ago when you first began to tutor me in Ochem. I knew then that I had one of the most amazing brothers anyone could ask for. You have guided me all the way, from phone calls about polymer chemistry to hard lessons of life. You continue to inspire me. Michael, you have taught me to never give up, no matter what society might say or dictate. I must say the same to you. Don't ever give up! I love you.

To my father, Larry. Dad, thank you for your continued support over the years. You have never given up on me. I would call home wanting to just quit and with your help I never gave in. You have taught me to face my challenges head on and figure out a way to overcome anything in my path. What is that phrase you continuously repeat, "Life isn't fair." No Dad, life isn't fair, but because of the lessons you have taught me, life is a little easier. From scoring goals in soccer to graduating with a master's degree, you have never stopped cheering for me. As I embark on my journey into the U.S. Navy, I hope to be as good as an officer as you once were. I want to model my approach, attitude, work

ethic, and commitment as an U.S. Naval Officer after you. You are the epitome of a true Naval Officer. GO NAVY!!! (But I will always be a Hokie first!) I love you.

Finally, I want to thank my mother, Patricia. Above everyone else thanked in this list, you are certainly the most important. You have truly been my inspiration since a young lad. You have taught me to never, never give up. Mom, with out you, none of my accomplishments would have been possible. You have truly been my rock and voice of guidance. You have been absolutely the best Mom a kid could ask for. Never once thinking of yourself and putting your children and me first. There is no award in the world that could honor your sacrifice and determination to make all of us to succeed. However, I can dedicate this master's to you. Mom, throughout all my education I have struggled to truly find out what career path I wanted embark upon. Through endless conversations, phone calls, and simple dinners with you and Dad, I believe I am truly ready to be an officer in the U.S. Navy. Mom this master's is a testament to all your hard work and unconditional love and support. Thank you Mom and Go Navy!!!! I love you so much. Please don't ever let up on me!!!!

**Table of Contents**

**Abstract** ... ii
**Acknowledgments** ... iii
**Table of Contents** ... v
**Abbreviations** ... viii
**List of Figures** ... ix
**List of Tables** ... xi
**1. CHAPTER 1: Thesis Overview** ... 1
**2. CHAPTER 2: Review: Block Copolymers in Drug Delivery** ... 3
**2.1. Abstract** ... 3
**2.2. Introduction** ... 3
**2.3. Synthesis and Preparation of Drug-Loaded Polymeric Micelles** ... 5
2.3.1. Synthesis of Poly(ethylene oxide-b-lactide)Copolymers and Micelles ... 6
2.3.2. Synthesis of Poly(ethylene oxide-b-β-benzyl L-aspartate) (PBLA) Copolymers and Micelles ... 8
**2.4. Synthesis and Preparation of pH Sensitive Block Copolymers** ... 9
2.4.1. Synthesis of Poly(ethylene oxide-b-(2-aminoethyl)aspartamide) ... 10
2.4.2. Synthesis of poly(ethylene oxide-b-3-{[({[hydrazino carbonyl]methyl}sulfanyl)propoxy}methyl}oxirane) ... 12
**2.5. Synthesis and Preparation of Ionically Stabilized Polymeric Micelles for Drug Loading** ... 14
2.5.1. Synthesis of poly(ethylene oxide-b-(2-methacryloyloxy)ethyl phosphorylcholine-b-2-diethylaminoethyl methacrylate) copolymers and micelle 15
**2.6. Synthesis and Preparation of Pluronic Block Copolymers for Drug Delivery** ... 18
2.6.1. Characteristics and Cytotoxicity of Pluronics™ ... 19
**2.7. Conclusions** ... 21
**3. CHAPTER 3: Synthesis and Characterization of Polyether-Polyacrylate Block Copolymers** ... 22
**3.1. Abstract** ... 22
**3.2. Introduction** ... 22
**3.3. Materials** ... 25
3.3.1. Chemicals ... 25
3.3.2. Solvents ... 26
**3.4. Characterization** ... 26
**3.5. Synthesis of Poly(*tert*-butyl acrylate) Homopolymers** ... 27
3.5.1. Synthesis of Poly(*tert*-butyl acrylate) in Acetone ... 27
3.5.2. Synthesis of Poly(*tert*-butyl acrylate) in Toluene ... 28
**3.6. Synthesis of Poly(ethylene oxide-*b*-propylene oxide-*b*-ethylene oxide)** ... 28
3.6.1. Synthesis of Poly(propylene oxide) Initiated by 1,12-dodecanediol ... 29
3.6.2. Preparation of Potassium Naphthalide Solution ... 29
3.6.3. Synthesis of Poly(ethylene oxide-*b*-propylene oxide-*b*-ethylene oxide) ... 30
**3.7. Synthesis of Polyether-Polyacrylate Block Copolymers** ... 31
3.7.1. Bromination of HO-PEO-PPO-PEO-OH ... 31
3.7.2. Synthesis of Poly(tert-butyl acrylate-b-ethylene oxide-b-propylene oxide-b ethylene oxide-b-tert-butyl acrylate) ... 31

3.7.3. Bromination of Pluronic P85, HO-$PEO_{26}$-$PPO_{41}$-$PEO_{26}$-OH ..... 32
3.7.4. Synthesis of $PtBA_{27}$-$PEO_{26}$-$PPO_{41}$-$PEO_{26}$-$PtBA_{27}$ ..... 33
3.7.5. Deprotection of $PtBA_{27}$-$PEO_{26}$-$PPO_{41}$-$PEO_{26}$-$PtBA_{27}$ ..... 34
3.7.6. Bromination of 2,000 g $mol^{-1}$ $CH_3$-PEO-OH ..... 34
3.7.7. Synthesis of Poly(ethylene oxide)-b-poly(tert-butyl acrylate) Diblock ..... 35
3.7.8. Deprotection of $CH_3O$-$PEO_{45}$-$PtBA_{117}$ ..... 36
**3.8. Results and Discussions of the Polyether-Polyacrylate Block Copolymers. 37**
3.8.1. Results and Discussion of the homopolymeriztion of tert-butyl acrylate ... 37
3.8.2. Results and Discussion of HO-PEO-PPO-PEO-OH ..... 38
3.8.3. Results and Discussion of Br-PEO-PPO-PEO-Br ..... 41
3.8.4. Results and Discussion of PtBA-PEO-PPO-PEO-PtBA ..... 41
3.8.5. Results and Discussion of Br-$PEO_{26}$-$PPO_{41}$-$PEO_{26}$-Br ..... 43
3.8.6. Results and Discussion of $PtBA_{27}$-$PEO_{26}$-$PP41_7$-$PEO_{26}$-$PtBA_{27}$ ..... 43
3.8.7. Results and Discussion of $PAA_{27}$-$PEO_{26}$-$PP41_7$-$PEO_{26}$-$PAA_{27}$ ..... 45
3.8.8. Results and Discussion of $CH_3O$-$PEO_{45}$-Br ..... 46
3.8.9. Results and Discussion of $CH_3O$-$PEO_{45}$-$PtBA_{117}$ ..... 47
3.8.10. Results and Discussion of $CH_3O$-$PEO_{45}$-$PAA_{117}$ ..... 48
3.8.11. Summary of Results of Polyether-polyacrylate block copolymers ..... 49
**3.9. Conclusions ..... 50**
**4. CHAPTER 4: Release Studies of Gentamicin from Block Ionomer-Antibiotic Nanoplexes as a Function of pH ..... 51**
**4.1. Abstract ..... 51**
**4.2. Introduction ..... 51**
**4.3. Experimental ..... 54**
4.3.1. Materials ..... 55
4.3.2. Characterization ..... 55
4.3.3. Preparation of Buffer Solutions ..... 55
4.3.3.1. Preparation of Phosphate Buffer Solution, pH 7.4 ..... 55
4.3.3.2. Preparation of Borate Buffer Solution, pH 9.7 ..... 56
4.3.4. Fabrication of Polymer-Antibiotic Nanoplexes ..... 56
4.3.4.1. Fabrication of Polymer-Antibiotic Nanoplexes Via a Batch Method ..... 56
4.3.4.2. Fabrication of Polymer-Antibiotic Nanoplexes Via a Continuous Engineering Method ..... 57
4.3.4.3. Isolation of Polymer-Antibiotic Nanoplexes ..... 58
4.3.5. Measurement of Gentamicin Release for Assaying Gentamicin ..... 59
4.3.5.1. Constructing a Calibration for Assaying Gentamicin ..... 59
4.3.5.2. Release Protocols for Polymer-Antibiotic Nanoplexes as a Function of pH ..... 60
4.3.5.2.1. Release Studies at pH 7.4 ..... 60
4.3.5.2.2. Release Studies at pH 4.5 ..... 60
**4.4. Results and Discussions ..... 61**
4.4.1. Comparison of the Batch and Continuous Fabrication Methods ..... 61
4.4.2. Comparison of Release Efficiencies of Gentamicin from the Nanoplexes at pH 7.4 ..... 65
4.4.3. Comparison of Release Efficiencies of Gentamicin from the Nanoplexes at

pH 4.5 ..... 67
**4.5. Conclusions ..... 69**
**5. CHAPTER 5: Conclusions ..... 71**
**5.1. Summary ..... 71**
**5.2. Conclusions ..... 72**
**REFERENCES ..... 74**

**Abbreviations**

ATRP – atom transfer free radical polymerization
Cu(I)Br – copper (I) bromide
$Cu(II)Br_2$ – copper (II) bromide
DI – deionized
DLS – dynamic light scattering
DOX - doxorubicin
EO – ethylene oxide
$^1H$ NMR – proton nuclear magnetic resonance
mL - milliliter
$M_N$ – number average molecular weight
Mol – mole
MWCO – molecular weight cut-off
PAA – poly(acrylic acid)
PBS – phosphate bufferred saline
PEO – poly(ethylene oxide)
PDI – polydispersity index
PMDETA – pentamethyldiethylenetriamine
PPM – parts per million
PPO – poly(propylene oxide)
PO – propylene oxide
PtBA – poly(*tert*-butyl acrylate)
RAFT – reversible addition-fragmentation chain transfer polymerization
SEC – size exclusion chromatography
tBA – *tert*-butyl acrylate
THF - tetrahydrofuran
UV-Vis spectroscopy– ultraviolet visible spectroscopy
μg - microgram

**List of Figures**

**Figure 2.1.** Illustration of a core-shell micelle ..... 5

**Figure 2.2.** Ring opening polymerization of ethylene oxide under basic conditions ..... 7

**Figure 2.3.** Ring opening polymerization of D,L-lactide utilizing $CH_3$-PEO-$O^{-+}K$ as the macroinitiator ..... 7

**Figure 2.4.** Polymerization of β-benzyl L-aspartate *N*-carboxyanhydride utilizing amino-terminated poly(ethylene oxide) ..... 8

**Figure 2.5** Chemical conjugation of PEO-PAsp with doxorubicin ..... 9

**Figure 2.6.** Removal of the benzyl group with ethylenediamine to form poly(ethylene oxide-*b*-(2-aminoethyl)aspartamide) ..... 11

**Figure 2.7.** Chemical functionalization of poly(ethylene oxide-*b*-(2 aminoethyl)aspartamide) ..... 12

**Figure 2.8.** Synthesis of poly(ethylene oxide)-*b*-poly(allyl glycidyl ether) ..... 13

**Figure 2.9**. Chemical conjugation of doxorubicin via a hydrazone linkage ..... 14

**Figure 2.10.** Structure of poly[2-(methacryloyloxy)-ethyl phosphorylcholine]-*b*-poly[2 (diethylamino)-ethyl methacrylate] ..... 16

**Figure 2.11.** Subsequent polymerization of DEA via atom transfer radical polymerization ..... 17

**Figure 2.12.** General structure of Pluronics™: poly(ethylene oxide-*b*-propylene oxide-*b* -ethylene oxide) ..... 18

**Figure 2.13.** Step-wise synthesis of Pluronics™: poly(ethylene oxide-*b*-propylene oxide-*b* -ethylene oxide) ..... 19

**Figure 3.1.** Polymerization techniques and correlation of degrees of polymerization and monomer conversion ..... 23

**Figure 3.2.** Typical ATRP reaction mechanism ..... 24

**Figure 3.3.** $^1$H NMR of methyl 2-bromopropionate ..... 37

**Figure 3.4.** $^1$H NMR spectra showing homopolymerizations of *tert*-butyl acrylate in acetone and toluene ..... 38

**Figure 3.5.** $^1$H NMR of 1,12-dodecandiol for initiation of PO ..... 39

**Figure 3.6.** (a) $^1$H NMR spectra of PPO initiated with 1,12-dodecanediol, and (b) macroinitiation of EO with PPO ..... 40

**Figure 3.7.** Bromination of HO-PEO-PPO-PEO-OH utilizing 2-bromoisobutyryl bromide ..... 41

**Figure 3.8.** Representative $^1$H NMR spectrum of polymerization of *tert*-butyl acrylate utilizing Br-PEO-PPO-PEO-Br ..... 42

**Figure 3.9.** SEC chromatogram of the precursor HO-PEO-PPO-PEO-OH ..... 43

**Figure 3.10.** $^{1}$H NMR spectrum of a brominated 4,600 g mol$^{-1}$ Pluronic P85™ polyether ..... 43

**Figure 3.11.** $^{1}$H NMR spectrum of the polymerization of *tert*-butyl acrylate using brominated P85 ..... 44

**Figure 3.12.** SEC chromatograms of Pluronic P85™ and P85-PtBA..... 45

**Figure 3.13.** $^{1}$H NMR of a deprotected polyether-poly(acrylic acid) pentablock copolymer ..... 46

**Figure 3.14.** Representative $^{1}$H NMR spectrum of a brominated 2,000 g mol$^{-1}$ PEO homopolymer ..... 47

**Figure 3.15.** Representative $^{1}$H NMR spectrum after the polymerization of *tert*-butyl acrylate using a 2,000 g mol$^{-1}$ PEO macroinitiator..... 48

**Figure 3.16.** Representative $^{1}$H NMR spectrum of a deprotected polyether-polyacrylate diblock copolymer ..... 49

**Figure 4.1.** Ionic condensation of cationic gentamicin with anionic polyether-polyacrylate block copolymers ..... 52

**Figure 4.2.** Schematic representation of a multi-inlet vortex mixer ..... 54

**Figure 4.3.** Synthetic scheme of the reaction of the primary amines of gentamicin with phthalaldehyde and mercaptoethanol..... 64

**Figure 4.4.** Gentamicin calibration curve..... 65

**Figure 4.5.** Release of gentamicin at pH 7.4 from nanoplexes prepared in a batch method..... 66

**Figure 4.6.** Release efficiencies at pH 7.4 of gentamicin from nanoplexes prepared in a continuous engineering process ..... 67

**Figure 4.7.** Release of gentamicin at pH 4.5 from nanoplexes made through a batch method..... 68

**Figure 4.8.** Release of gentamicin at pH 4.5 from nanoplexes prepared in a continuous engineering process ..... 69

**Figure 4.9.** Titration curve of poly(acrylic acid) utilizing a strong base ..... 69

**List of Tables**

**Table 3.1.** Homopolymerizations of *tert*-butyl acrylate in acetone and toluene ..... 38

**Table 3.2.** Summary of polyether polyacrylate block copolymers and PtBA homopolymers ..... 49

**Table 4.1.** Summary of data compiled from the fabrication of polymer-antibiotic nanoplexes via continuous and batch processes ..... 61

**Table 4.2.** Summary of data of the size distributions of nanoplexes from each fabrication technique ..... 62

**Table 4.3.** Comparison of loading capacities of gentamicin through both fabrication methods ..... 65

## Chapter 1: Thesis Overview

Many pathogenic bacteria can enter immune cells and replicate in them. These intracellular bacteria are difficult to treat because they can evade the host's defenses. Specifically, Gram-negative food-borne bacteria, such as *brucella*, *salmonella*, and *listeria*, have this type of replication mechanism. Current antibiotics used to treat Gram-negative bacterial infections include gentamicin sulfate, among the aminoglycoside class of antibiotics.[1]

Gentamicin is a compound composed of three sugar groups and five amino groups. At physiological pH the amino groups are protonated and the drug has an overall positive charge. Polar antimicrobials do not substantially transport through hydrophobic cell membranes because the positive charges inhibit uptake of the antibiotic into the target cells.[2] As a result, free gentamicin introduced as the gentamicin sulfate salt has limited antimicrobial effect on intracellular bacteria.

Drug encapsulation through cooperative electrostatic attractions with a polymeric carrier can be an effective design to increase drug accumulation within the target location. Nonionic-anionic polyether-polyacrylate block copolymers can encapsulate gentamicin. Through an ionic condensation, the cationic drug can be bound to the anionic polyacrylate blocks. As a result, a core-shell polymeric micelle is created that houses a charged core containing a complementary charged drug and a nonionic polyether shell.

This thesis examines the formation of polymer-antibiotic nanoplexes and release of the drug at pH 7.4 (to simulate physiological pH) and pH 4.5 (to simulate endosomal pH). Polyether-polyacrylate diblock and pentablock copolymers were synthesized by

controlled radical polymerization (ATRP). Two fabrication methods for making the nanostructures were compared: a batch method and a continuous engineering method. The batch method was conducted by adding a solution of the drug salt dropwise to a polymer solution, and the continuous process relied on rapid turbulent mixing of solutions of the polymers and drug salt as they entered the mixing chamber. In the batch method, the ratio of drug-to-polymer increased during the addition, while the continuous method was conducted such that the drug-to-polymer ratio remained constant throughout the process. The rates and efficiencies of drug release from these nanoplexes was investigated as a function of pH. It was hypothesized that the continuous process would produce a more steady release of gentamicin due to better homogeneity of the nanoplexes.

# CHAPTER 2: Review: Block Copolymers in Drug Delivery

T. P. Vadala

*Macromolecules and Interfaces Institute,*
*Virginia Polytechnic Institute and State University,*
*Blacksburg, VA 24061-5976, USA*

## 2.1 Abstract

Block copolymers are employed extensively in the area of drug delivery due to their excellent chemical and biological properties. They are designed to be pH sensitive, biodegradable, photochemically active, cationic, anionic, or amphiphilic. These properties can be controlled by the selection of the monomeric species, chemical post-modifications of the copolymeric moiety, and cross-linking block copolymers. The main biomedical objective of these block copolymers is the controlled release of various pharmaceuticals. This review discusses the synthesis and application of block copolymers in polyionic, biodegradable, pH sensitive, Pluronic-based, and drug-loaded polymer micelles.

Keywords: Block copolymers, drug delivery, biodegradable, amphiphilic, polyionic, micelles

## 2.2 Introduction

Recently, block copolymers have been employed in drug delivery due to their excellent chemical and biological properties.[3-6] These properties can be manipulated to design the most optimal candidate for drug delivery. Among these properties, the block copolymers should have good biocompatibility. They must meet the criteria of the human body and not cause any harm to the individual, such as triggering an immune

response. In addition, the polymers must be capable of delivering the drug in a controlled fashion. It is desirable for the polymer to transport the drug to the desired site in the body, and release the drug on a schedule commensurate with the desired treatment protocol.

There are many ways to deliver a drug, protein, or polynucleotide using polymer carriers. Amphiphilic block copolymers can form micelles in an aqueous environment, where the core is hydrophobic and the shell is hydrophilic. This is especially important because many drugs are hydrophobic and thus have poor solubility in water. Encapsulating the drug in a hydrophobic core which is surrounded by a hydrophilic shell can increase the efficiency of delivery by helping to disperse or solubilize the constructs.

The natural environments within the human body can be used to stimulate the polymer to release the drug, for example, the vast pH ranges of the human body. The gastrointestinal tract alone changes from pH 6.5 in the oral cavity to pH 1.0 to 2.0 in the stomach. The pH of the blood stream is 7.4 and within an endosome is less than pH 5.0. Polymers can be designed to match these environments and respond accordingly to release their payload.

Discussed in this review are ways to increase the efficiency of drugs through the use of block copolymers. Specifically, this review discusses the synthesis and preparation of polymer micelles. These micelles can be formed through hydrophobic forces, as observed for poly(ethylene oxide-*b*-lactide) (PEO-PLA) block copolymers and poly(ethylene oxide-*b*-propylene oxide-*b*-ethylene oxide) copolymers (i.e., Pluronics™), and through cooperative electrostatic attractions between a drug and a polymer having complementary charges. Additionally, this review discusses the synthesis and

preparation of pH sensitive block copolymers. These polymer-drug complexes are stable at physiological pH, but become unstable at lower pH levels.

**2.3 Synthesis and Preparation of Drug-Loaded Polymeric Micelles**

Polymer micelles possess a core-shell architecture that contains a segregated hydrophobic core surrounded by a hydrophilic shell, as depicted in figure 2.1.[7] In terms of drug delivery, the hydrophobic core is important because of the potential for loading hydrophobic drugs and solubilizing them in aqueous media.[8] Most pharmaceuticals are hydrophobic; therefore, hydrophobic interactions are utilized as the main source of polymer-drug incorporation.[3-6] However, electrostatic, π-π bonding, and hydrogen bonding interactions have also been used in the formation of polymer micelles.[9-11] In addition to the hydrophobic core, the hydrophilic shell also plays a vital role in the formation of these micelles. The hydrophilic shell supplies the steric or electrostatic repulsion of individual particles and improves micellar solubility in an aqueous environment.[12,13]

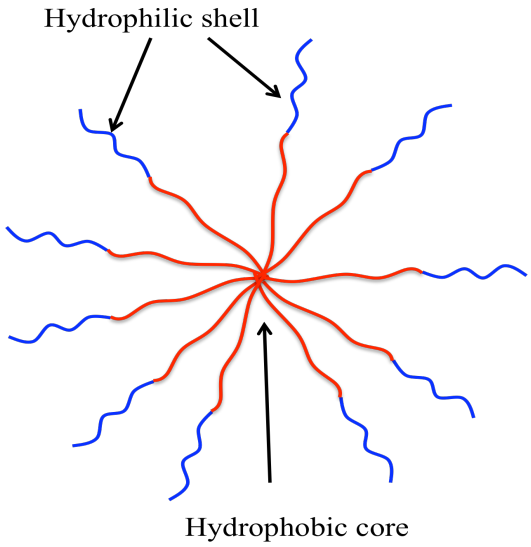


Figure 2.1: Illustration of a core-shell micelle. The hydrophobic polymers aggregate to the center and are surrounded by the hydrophilic polymers

Typically, polymer micelles utilize an AB or ABA type block copolymer architecture.[14] Incorporating graft or multi-segmented block copolymers into the micellar system can add new variables that change the formation and characteristics of these polymeric micelles.[14] As a result, drugs can be incorporated into the core of the micelle in at least two ways: physical entrapment or covalent bonding. During micelle formation, the drug can be encapsulated within the core due to hydrophobic interactions between drug and polymer.[15] In contrast, covalent bonding can be used as a means to bind the drug to the polymer. The drug can be chemically conjugated through linking molecules, then degradation through the linkers can be an important source of drug release. Once the micelle arrives at the target location, the linkers can be activated by local stimuli such as ions, enzymes, or pH differences.[16]

*2.3.1 Synthesis of Poly(ethylene oxide-b-lactide)Copolymers and Micelles*

Polylactides have been used in biomedicine and commercialized as surgical sutures and microspheres for controlled drug delivery.[8] The chemical lability of polylactides results in degradation through ester hydrolysis. Lactides have been copolymerized with other monomers to modulate the block copolymers' mechanical, physical, and degradation properties. One major class of block copolymers containing polylactides that is utilized in biomedicine is PEO-PLA. PEO is non-toxic and non-immunogenic.[17] Additionally, PEO increases the overall hydrophilicity of the copolymer and can be excreted by the kidneys under a critical molecular weight of ~50,000 g $mol^{-1}$.[18]

Yagusi et al. produced a PEO-PLA block copolymer in a multi-step polymerization, as depicted in figures 2 and 3.[8] First, a ring-opening polymerization was

performed using ethylene oxide. The reaction proceeded under living conditions in a basic environment with 2-methoxyethoxide as the initiator at room temperature (figure 2.2).

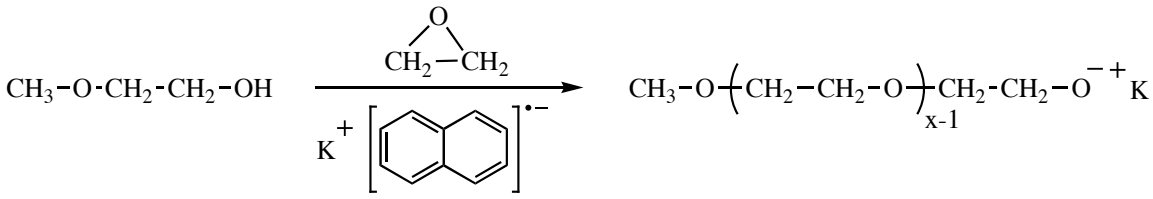

Figure 2.2: Ring opening polymerization of ethylene oxide under basic conditions

The resulting polymer, $CH_3O$-PEO-OH, was precipitated into an excess of diethyl ether and dried under reduced pressure. The PEO segment was characterized by GPC and yielded a low molecular weight distribution of 1.05.[8] $CH_3O$-PEO-OH was utilized as a macroinitiator in the subsequent ring-opening polymerization of D,L-lactide. This reaction was also performed under basic conditions, as shown in figure 2.3.

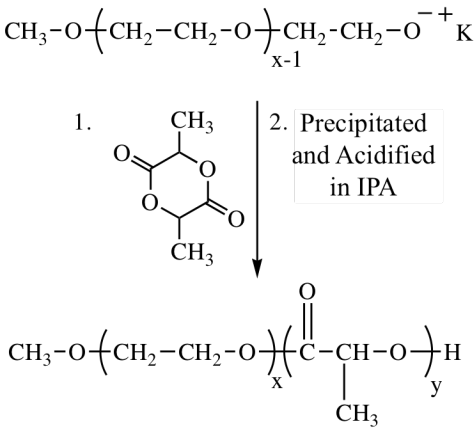


Figure 2.3: Ring opening polymerization of D,L-lactide utilizing $CH_3$-PEO-O-+K as the macroinitiator

The resulting block copolymer was precipitated in isopropanol, acidified, and dried under reduced pressure. The overall combination of PEO and PLA is an excellent candidate for drug delivery due to the resulting amphiphilicity of the block copolymer. PEO is hydrophilic whereas PLA is hydrophobic. Thus, in aqueous media, the PEO-PLA copolymers form micelles through multi-molecular association.[19] The hydrophobic core

is an excellent candidate for encapsulation of a hydrophobic drug. These block copolymers can deliver hydrophobic drugs through dispersion in aqueous media, and release the drug through hydrolysis of the ester bonds.

*2.3.2 Synthesis of Poly(ethylene oxide-b-β-benzyl L-aspartate) (PBLA) Copolymers and Micelles*

PEO can also be copolymerized with a hydrophobic poly(amino acid). The hydrophobic poly(amino acid) and hydrophilic PEO form micelles in aqueous media. One important issue for PEO-*b*-PBLA copolymer micelles is the molecular weight ratios of PEO to PBLA. Changing the ratio alters the hydrophobic to hydrophilic balance. This controls the overall amphiphilicity, which can affect the loading capacity of the desired drug.[20-22] As depicted in figure 2.4, an amino-terminated PEO has been utilized to initiate the ring-opening polymerization of β-benzyl L-aspartate *N*-carboxyanhydride in DMF.[23]

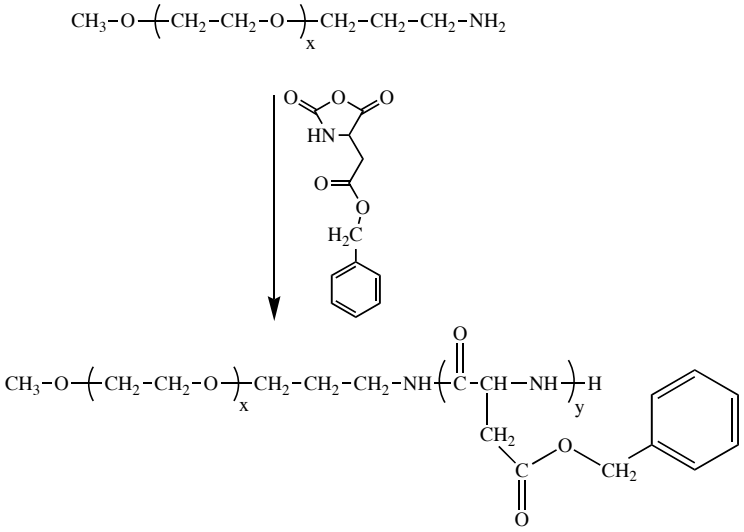

Figure 2.4: Polymerization of β-benzyl L-aspartate *N*-carboxyanhydride utilizing amino-terminated poly(ethylene oxide)

Polymer micelles comprised of these block copolymers were utilized to physically encapsulate and also chemically-bond adriamycin or doxorubicin.[23] Drug encapsulation

was accomplished during micelle formation. If the micelles were formed before drug encapsulation, then the loading efficiency decreased and the particle size became larger with a broader size distribution.[23] Physical entrapment of doxorubicin, however, showed low micelle stability due to poor affinity of the PBLA segment with doxorubicin. As a result, the PEO-PBLA block copolymer was chemically modified to bond to doxorubicin, as shown in figure 2.5.[23]

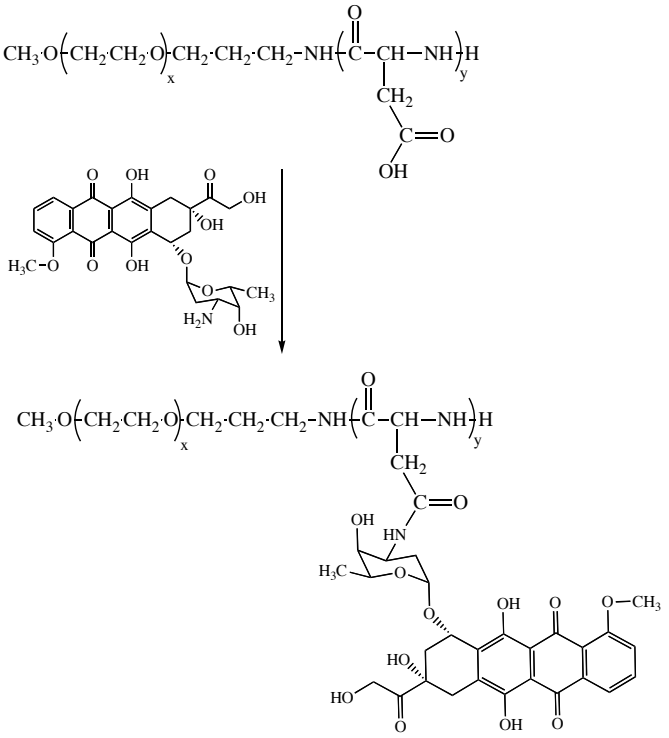

Figure 2.5: Chemical conjugation of PEO-PAsp with doxorubicin

Poly(β-benzyl L-aspartate) was deprotected with acid to yield poly(aspartic acid). Doxorubicin was conjugated to the side chain of poly(aspartic acid) using its primary amino group and the polymer's carboxylic acid group.[24,25] The loading efficiency increased from 10 to 65 percent as a result of the change of method for drug loading. Fifty percent of all carboxylate groups were conjugated with doxorubicin.

**2.4 Synthesis and Preparation of pH Sensitive Block Copolymers**

"Smart" polymers are polymers that change their structural properties in response to an external stimulus, such as pH, temperature, or light.[14] Recently, these smart polymers have been used in a wide variety of applications, including bioactive agent delivery.[26, 27] pH sensitive block copolymers are of interest because they can adjust to the vast pH range of the body.[28] In general, the pH of the blood stream is 7.4 whereas the pH within cells varies and can be lower than pH 5.0. The most significant change in pH within the human body occurs in the gastrointestinal tract. From the point of oral ingestion, the pH begins at 6.5 and drops dramatically to pH 1.0-2.0 within the stomach, then increases to 4.0-5.5 in the intestinal tract.[14]

Accordingly, these block copolymers must possess certain chemical components that change with the pH of the biological environment and take advantage of these variations, whether they occur naturally or under pathological conditions. These components are normally designed to be stable at neutral and basic pH, but become unstable in acidic environments. A list of some chemical components that are susceptible to changes with pH include acetals, hydrazones, carboxylates, sulfonates, and orthoesters.[28] Esters and amides with β-hydroxy groups have been less studied, but also fall in this category.

*2.4.1 Synthesis of Poly(ethylene oxide-b-(2-aminoethyl)aspartamide)*

Lee et al. utilized a direct approach to pH sensitive block copolymers.[28] Their main objective was to couple a block copolymer with a short chain protein. The target biological location of the protein was an endosome with a pH of approximately 5.0.[28] They utilized citraconic anhydride, an α-methyl derivative of maleic anhydride, conjugated to poly(ethylene oxide-*b*-β-benzyl L-aspartate). The synthesis began with the

ring-opening polymerization of β-benzyl L-aspartate *N*-carboxyanhydride (as in figure 2.4).[29] The subsequent reaction involved removing the β-benzyl group with ethylenediamine (figure 2.6). At room temperature in DMF, the block copolymer solution was added dropwise into an excess of ethylenediamine. This limited the amount of polymer coupling between chains. The product was precipitated into an excess of hexane/diethyl ether and dried under reduced pressure.

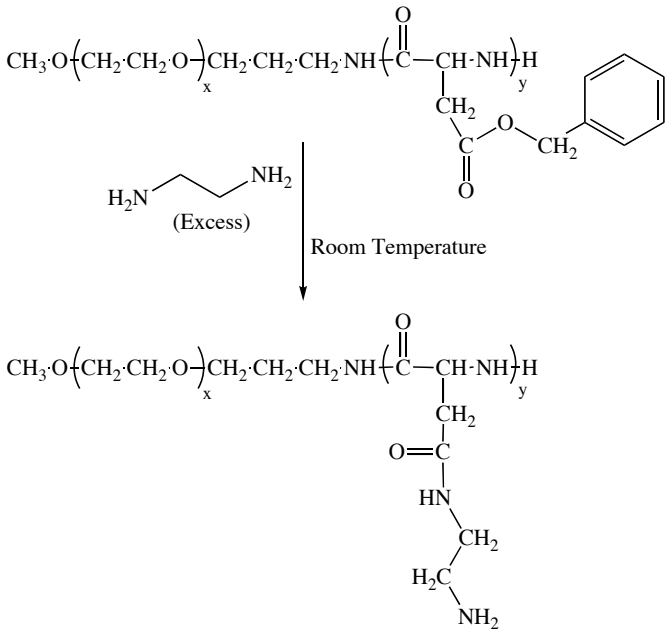


Figure 2.6: Removal of the benzyl group with ethylenediamine to form poly(ethylene oxide-*b*-(2-aminoethyl)aspartamide)

The next step involved the reaction of the new amino groups with citraconic anhydride (figure 2.7). Poly(ethylene oxide-*b*-(2-aminoethyl)aspartamide) was dissolved in pyridine and reacted with citraconic anhydride at room temperature.

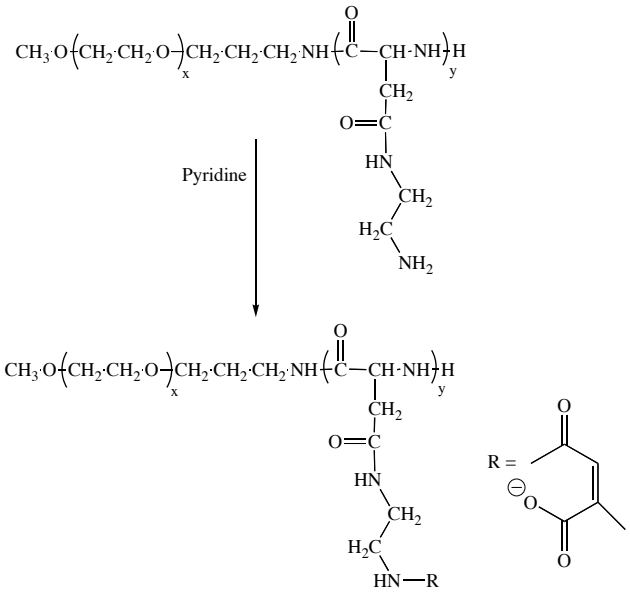


Figure 2.7: Chemical functionalization of poly(ethylene oxide-*b*-(2-aminoethyl)aspartamide)

Citraconic amide is stable at both neutral and basic pH; however, the carboxylic acid deprotonates at acidic pH's, becoming negatively charged. As a result, these negative carboxylate groups make excellent candidates for drug loading. The block copolymer was utilized to carry proteins by generating an electrostatic force between the positively charged lysine groups of a protein and the negative carboxylate groups. Lee et al. studied degradation rates of the citraconic amide via a fluorescamine method, which measured the amine concentration.[28] In an acetate buffer (pH 5.5), 80% of the citraconic amides were degraded within one hour, whereas in phosphate buffer (pH 7.4), 60% of the citraconic amides remained intact after five hours. These results showed that the citraconic amide is fairly stable at physiological pH but begins to degrade at low pH. Within an endosome, the polymeric micelles would begin to dismantle due to core degradation at the lower pH, thus releasing the protein.

*2.4.2 Synthesis of poly(ethylene oxide-b-3-{[({[hydrazino-carbonyl]methyl}sulfanyl)propoxy}methyl}oxirane)*

Hruby et al. utilized hydrazone linkages that were sensitive to pH for drug delivery.[30] The copolymer synthetic pathway proceeded via a ring-opening polymerization of allyl glycidyl ether (figure 2.8). The polymerization utilized sodium hydride as the base to form an alkoxide from monomethoxy-functional poly(ethylene oxide) under a nitrogen atmosphere. Allyl glycidyl ether was charged to the reaction flask and reacted. The isolated poly(ethylene oxide-b-allyl glycidyl ether) was dried under reduced pressure, and passed through a silica column to remove impurities (side reactions from the polymerization). The polymerization of allyl glycidyl ether utilizing PEO had a 48 % yield. GPC results showed a narrow molecular weight distribution and a PDI of 1.05. GPC was performed in THF using PEO as the standards.

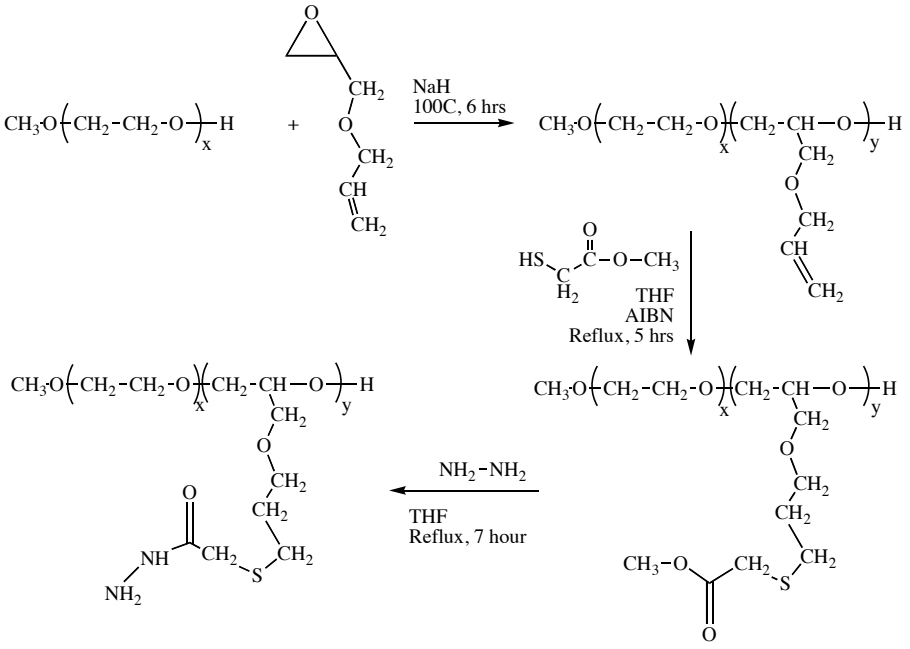


Figure 2.8: Synthesis of poly(ethylene oxide)-b-poly(allyl glycidyl ether)

The block copolymer was post-reacted with methyl sulfanylacetate in the presence of AIBN in an ene-thiol addition. The block copolymer was dissolved in THF and sulfanylacetate and AIBN were charged to the reaction flask. The reaction mixture

was stirred under reflux. Finally, the new ester group was modified with hydrazine hydrate (figure 2.9). The reaction proceeded in THF at reflux. The copolymer was freeze-dried under reduced pressure.

The hydrazone-functional block copolymer was finally reacted with doxorubicin. Doxorubicin and the poly(allyl glycidyl ether) formed the inner core of the polymer micelle with hydrophilic PEO blocks formed the shell. Results showed that the hydrazone linkage was relatively stable at neutral (physiological) pH, whereas the linkage began to cleave under slightly acidic environments, pH 5.0.[31] The doxorubicin released much faster at pH 5.0 than at pH 7.4.

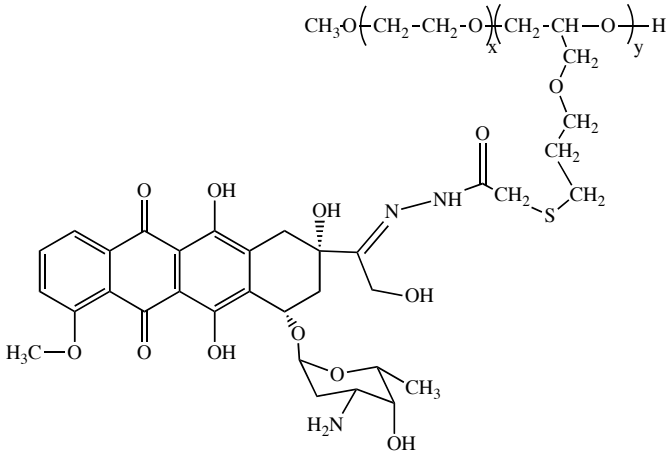

Figure 2.9: Chemical attachment of doxorubicin via a hydrazone linkage. At pH 5.0, this linkage will cleave, as the amine becomes protonated. The payload delivery is triggered by changes in pH.

## 2.5 Synthesis and Preparation of Polymeric Micelles for Gene Therapy

The potential capability to correct genetic disorders through gene therapy is of great interest.[32] Viral vectors have been one forefront of gene therapy. However, the utilization of block copolymers could aid in the delivery of genetic material or proteins. An advantage of block copolymers is that they can be tailored to avoid an immune

response by the host.[33-36] The polymer system must be able to deliver the DNA or protein in appropriate and controlled amounts. DNA has low gene transfection efficiency and cannot effectively traverse the cellular membrane.[34] Polymer micelles can be designed to be drug or gene carrying vesicles. Inherent to the properties of the micelles is the separation of the hydrophilic and hydrophobic portions. DNA is a negatively charged polynucleotide due to the anionic phosphate groups. Cationic polymers such as poly(L-lysine), polyethyleneimine and polyamidoamines all readily form complexes with DNA through electrostatic cooperation.[37-42]

*2.5.1 Synthesis of poly(ethylene oxide-b-(2-methacryloyloxy)ethyl phosphorylcholine-b-2-diethylaminoethyl methacrylate) copolymers and micelles*

Micelles must contain a hydrophilic and a relatively hydrophobic portion. Copolymerizing a cationic polymer with another hydrophilic block was shown to enhance the solubility and stability of the complex.[42,43] Zhao et al. investigated the loading and delivery efficacies of a triblock copolymer consisting of poly[2-(methacryloyloxy)-ethyl phosphorylcholine]-*b*-poly[2-(diethylaminoethyl) methacrylate] (PMPC-*b*-PDEA).

The first step of the synthesis utilized an atom transfer radical polymerization (ATRP) of 2-methacryloyloxyethyl phosphorylcholine (MPC) initiated by a brominated PEO macroinitiator (PEO-Br). In the presence of Cu(I)Br and a bpy ligand, PEO-Br was reacted with MPC in methanol (figure 2.10). The solution turned dark brown and progressively became more viscous.

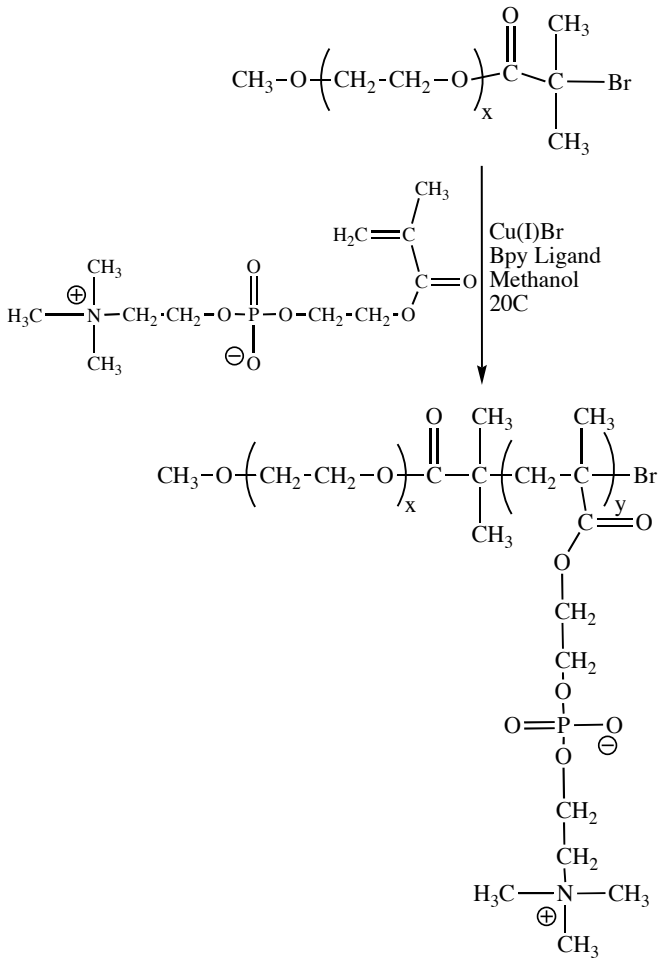


Figure 2.10: Structure of poly[2-(methacryloyloxy)-ethyl phosphorylcholine]-b-poly[2-(diethylamino)-ethyl methacrylate]

Towards the end of the polymerization of MCP, 2-diethylaminoethyl methacrylate (DEA) was injected into the flask and polymerized under the ATRP conditions (figure 2.11). The triblock was analyzed by size exclusion chromatography and found to have a $M_w/M_n$ of >1.20. GPC was measured using an aqueous phase against PEO standards with a refractive index detector.

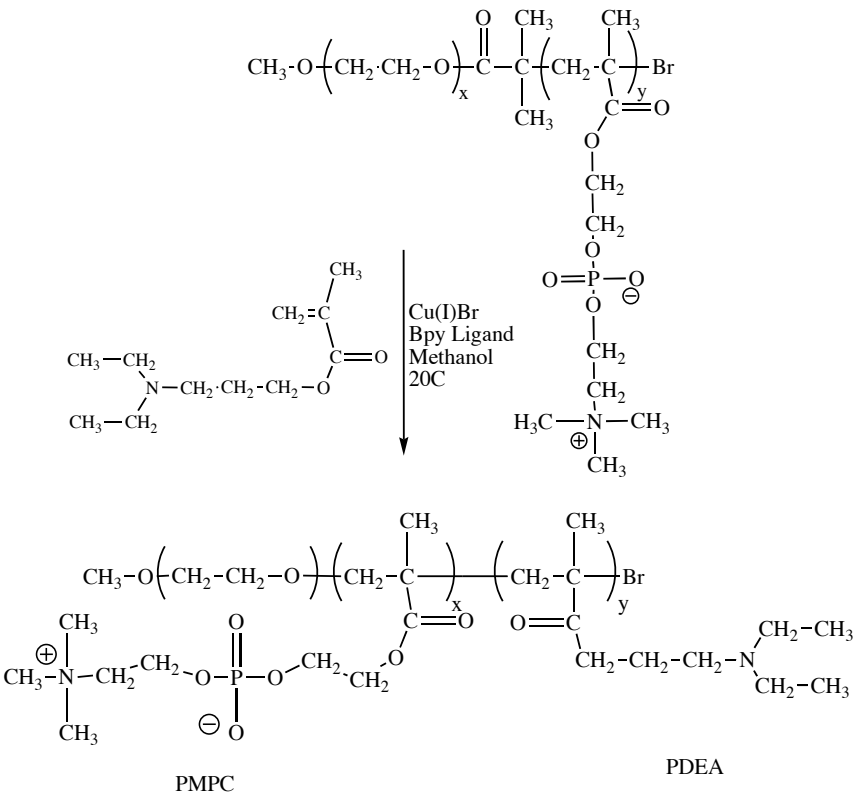


Figure 2.11: Block copolymerization of DEA via atom transfer radical polymerization

Zhao et al. showed that this novel copolymer could bind electrostatically to an oligonucleotide.[32] The polymer-oligonucleotide complex was soluble at pH 7 due to micelle formation of the charged core and the nonionic PEO hydrophilic shell. Cytotoxicity assays using HeLa cancer cells showed that the polymer complexes could transport the oligonucleotide into the cells. A negative control was used to show no transfection efficiency, whereas a positive control showed 95 % transfection efficiency (a commercial product). Transfection efficiencies were studied relative to the total number of cells. The polymer-oligonucleotide complex was tested in addition to each of the oligonucleotide and polymer separately. The results indicated that the electrostatically-bound polymer-oligonucleotide complex had better uptake than the oligonucleotide alone.

## 2.6 Synthesis and Preparation of Pluronic™ Block Copolymers for Drug Delivery

Synthetic block copolymers comprise the majority of materials utilized in drug and gene delivery.[44] Among these, Pluronics™ have been studied extensively in the past two decades in medicine and pharmaceutical sciences.[45-56] Pluronics™ are a family of polymers produced by BASF that consist of a poly(propylene oxide) (PPO) block flanked on either side by PEO blocks (figure 2.12). PEO is hydrophilic whereas PPO is relatively hydrophobic.

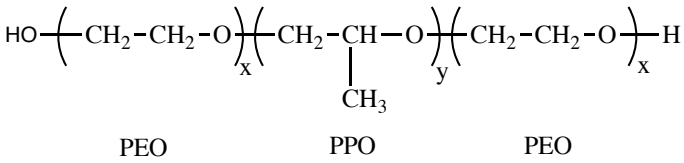


Figure 2.12: General structure of Pluronics™: poly(ethylene oxide-*b*-propylene oxide-*b*-ethylene oxide)

Changing the PEO to PPO ratio and/or the block lengths alters the overall amphiphilicity. Pluronics™ are synthesized under basic conditions starting with the polymerization of propylene oxide, then adding ethylene oxide by sequential addition (figure 2.13).

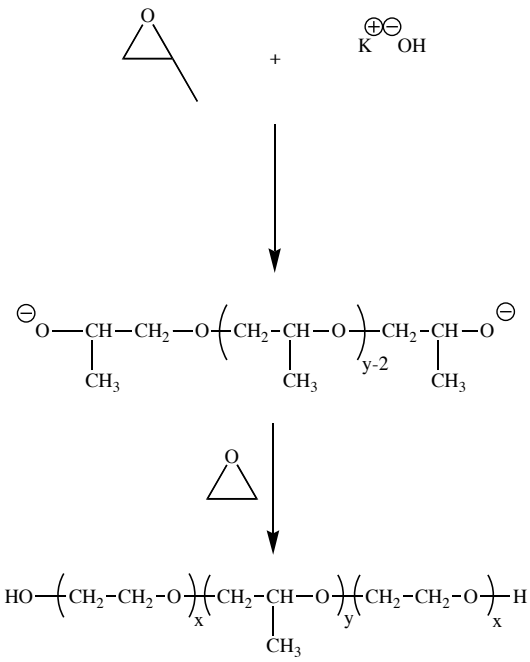

Figure 2.13: Step-wise synthesis of pluronics: poly(ethylene oxide-*b*-propylene oxide-*b*-ethylene oxide)

The hydrogens on the pendent methyl protons of PO are relatively acidic, and during the polymerization under basic conditions, side reactions with the PO monomer lead to allyl alkoxide side products that initiate polymerization. This produces a low molecular weight diblock polymer with an unsaturated allyl endgroup on one end. SEC curves show the presence of a low molecular weight shoulder on the main peak corresponding to the triblock that is consistent with a mixture of triblock and diblock architectures in these materials. Nevertheless, the amphiphilic nature of the Pluronics™ result in the formation of micelles in physiological media that are valuable as drug carriers.

*2.6.1 Characteristics and Cytotoxicity of Pluronics ™*

One characteristic of Pluronics™ is their capacity to form aggregates in aqueous media above a critical micelle concentration that comprise a dynamic mixture of micelles in equilibrium with unimers.[57] The driving force is the tendency for the PPO blocks to associate. These Pluronic-based micelles have the hydrophobic PPO in the core and the PEO forms a hydrophilic shell. The hydrophobic core is suitable for encasing

hydrophobic drugs such as doxorubicin. Pluronics™ have been shown to load low molecular weight hydrophobic drugs and polypeptides.[58]

Tumors with a multi-drug resistant (MDR) phenotype are among the most difficult cancer cells to treat.[59] These cancer cells are often associated with an over expression of a membrane-bound protein, P-glycoprotein (Pgp), that is involved in a transport system that pumps drugs out of the cell. This Pgp pump accounts for the low accumulation and retention of drugs in tumor cells.[60] The more Pgp proteins that are located on the tumor cell surface, the higher the probability for the drug to be pumped back out of the cell. As a result, Kabanov et al. and others have shown that Pluronics™ cannot carry drugs to the target location but have shown to deliver the drug. The Pluronic bypasses the P-glycoprotein pump and delivers the drug inside the cell.

Additionally, Pluronics™ have been shown to help increase the accumulation of doxorubicin in multi-drug resistant cells.[59] Normally, drugs used to treat these specific cells can be sequestered with cytoplasmic vesicles. The drugs are encapsulated within these vesicles and removed by the abnormally high activity of ATP-dependent efflux pumps.[61-65] This process depletes the drug from the target location, the cell nucleus. However, following incubation of the cells with doxorubicin and a Pluronic™ formulation, the drug released from the vesicles and accumulated near the nucleus.[59] These results indicate that the Pluronic™ protected the drug from cellular protein pumps by incorporating the hydrophobic drug into the core of the pluronic micelle.

However, these drug resistance systems that are over expressed on the multi-drug resistant cells, Pgp punps and ATP pumps require consistent energy to sustain their function. It was found that the polyether block copolymers caused a decrease in ATP

levels in the cells, and thus, less energy derived from ATP hydrolysis was available to activate the pump.[66,67] Pluronic P85 was utilized in this experiment to determine its effect on ATP levels in several different cell types, including cells with the multi-drug resistant phenotype. When tested against non-multi-drug resistant cells, no reduction in ATP levels was noticed. However, when tested against those cells with the multi-drug resistant phenotype, the ATP levels decreased.

**2.7 Conclusions**

This review discussed syntheses of block copolymers and their potential applications in drug delivery. The block copolymers form core-shell morphologies with a hydrophilic outer shell in aqueous media, and a hydrophobic or ionic core that is designed to bind to the drug through hydrophobic or electrostatic interactions, respectively. The block copolymers can include biodegradable components such as PEO-PLA that release the drug as the PLA core polymer degrades. They can comprise hydrophobic cores such as the PPO blocks of Pluronic™ triblock materials that bind to hydrophobic drugs through hydrophobic interactions and slowly release the cargo. They can have charged blocks that bind to drug or nucleic acids through complementary charge interactions. These can release the drug slowly due to disruption of the charges by salts or other charged species encountered in the physiological medium, or they could involve pH-sensitive cores that release due to a change in pH as the pH is lowered, for example, in an endosome. It has been shown that block copolymers have been tailored to be pH sensitive. The drug is either bound electrostatically or physically. The drug is usually bound to the block copolymer at neutral or basic pHs but is released from the polymer in more acidic environments.

# Chapter 3: Synthesis and Characterization of Polyether-Polyacrylate Block Copolymers

## 3.1 Abstract

Block copolymers are versatile in terms of their applications and chemical synthesis. Conventional free radical polymerizations have limitations that prevent the synthesis of homogeneous block copolymers. Usually, two monomers are polymerized simultaneously to yield a copolymer of a statistically random orientation. Another disadvantage is the premature termination of polymer chains during the reaction due to disproportionation and combination and the extreme reactivity of the free radical. However, if the radical can be controlled, conditions can be developed to prepare block copolymers. This chapter discusses atom transfer free radical polymerization and the polymerization of *tert*-butyl acrylate in the presence of a copper/ligand catalyst. *Tert*-butyl acrylate was polymerized using a small organic compound, methyl 2-bromopropionate, and several types of macroinitiators: HO-PEO-PPO-PEO-OH triblock, Pluronic P85, and a 2,000 g $mol^{-1}$ PEO homopolymer.

## 3.2 Introduction

Block copolymers are versatile in terms of their applications and chemical synthesis. They can be synthesized by step-growth and chain-growth pathways. Chain-growth reactions can be further separated in terms of the type of propagating species (radical, anion, cation, metal coordinated), and also by the degree of chemical and structural control over the reactions. Figure 3.1 shows a correlation between degrees of polymerization and conversion of monomer species. In step-growth polymerizations, small oligomers are created as a small amount of monomer is converted to polymer. The oligomers then combine over time to form longer chains. The polydispersity indices of polymers grown through this synthetic pathway approach 2.0. The progress of molecular weight increase in conventional free radical polymerizations is dictated by the relatively slow rates of initiation compared to propagation, and the fact that termination is not controlled. High degrees of polymerization are observed with low monomer conversion. These polymerizations undergo termination by disproportionation and chain combination,

and have polydispersity indices that range theoretically from 1.5-2.0 and that experimentally can be higher.

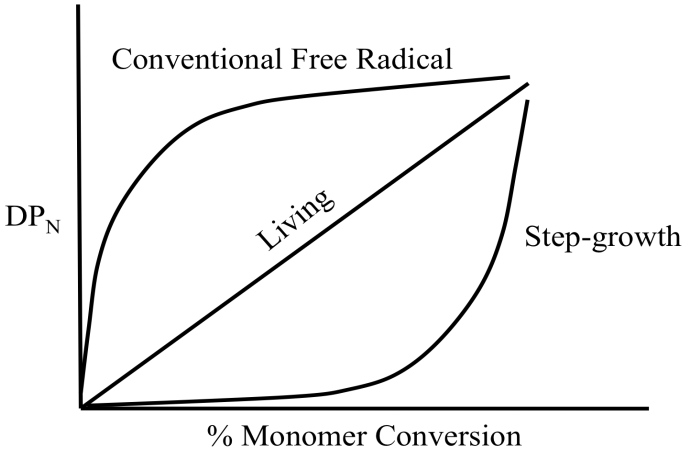


Figure 3.1: Polymerization techniques and corresponding correlation of degrees of polymerization and monomer conversion

Living anionic, and sometimes cationic, polymerizations are normally designed such that strong bases (or acids) are utilized as initiators and they are free from uncontrolled termination or chain transfer. If initiation is substantially faster than propagation, then all of the chains initiate early and this yields an approximately linear relationship between degree of polymerization and monomer conversion. The polydispersity indices approach 1.0 and the polymers are more homogeneous in terms of molecular weight. However, not all monomers are susceptible to living conditions. Monomer choice is very important and with that comes polymerization technique.

Controlled methods of free radical polymerizations have been of great interest for many years, and methods that approximate "living" conditions have been adapted to free radical pathways in attempts to limit premature termination and control molecular weights and polydispersities. In recent years, reversible addition-fragmentation chain transfer polymerization (RAFT) and atom transfer free radical polymerization (ATRP) have become increasingly important.[68-77] Both techniques allow for the controlled

polymerization of monomeric species usually polymerized by free radical processes. The key to decreasing the polydispersity of free radical polymerizations is to "control" reactivity and concentration of the radical.

Matyjaszewski and colleagues have made tremendous progress in developing ATRP to achieve "living" or controlled conditions for free radical pathways.[78] Figure 3.2 shows a typical synthetic scheme for an ATRP polymerization. The polymerization begins with the use of halogenated initiators, in this case a bromoalkane. The halogenated species can be a small organic molecule or a polymeric species. In either case, the carbon-bromine bond dissociates through reaction with a Cu(I)Br/ligand complex and produces a radical. This radical has two potential fates. It can react with a monomer or reduce the $Cu(II)Br_2$/ligand complex to reform the carbon-bromine bond. The persistent radical can be ultimately controlled and terminated with the final reduction of the $Cu(II)Br_2$/ligand complex.

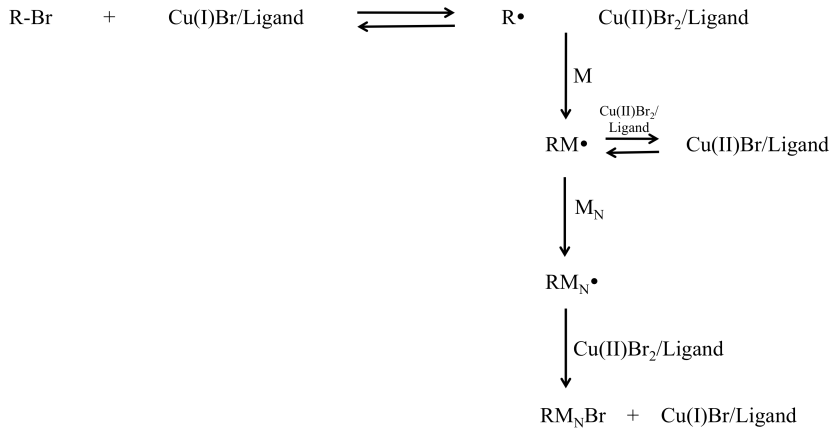


Figure 3.2: Typical ATRP reaction mechanism

In this chapter, ATRP was utilized to polymerize *tert*-butyl acrylate from the termini of difunctional polyether triblock copolymers and monofunctional PEO homopolymers. This monomer is especially important because the *t*-butyl groups can be removed to yield carboxylic acid groups. These carboxylic acid groups are deprotonated

at physiological pH yielding an anionic poly(sodium acrylate) block. The utilization of ATRP is vital to the formation of polymeric micelles of defined sizes and integrity. The overall goal of this research is to fabricate polymer-antibiotic nanoplexes. The complexes are held together electrostatically, through the binding of negatively charged polyether-polyacrylate block copolymers and a positively charged aminoglycoside, gentamicin. Controlling the lengths of the polyacrylates may be critical to the binding strength of the polymer to drug. ATRP was utilized to target a specific molecular weight of polyacrylate blocks.

This chapter will discuss the controlled radical polymerization of *tert*-butyl acrylate in the presence of small brominated organic initiators and brominated macroinitiators, such as PEO-Br and Br-PEO-PPO-PEO-Br. Additionally, this chapter discusses polymerizations of PO and EO. The resulting polyether triblock was utilized to improve our understanding of the ATRP limitations. All polyether-polyacrylate pentablocks and diblocks were synthesized and characterized by $^{1}$H NMR and size exclusion chromatography (SEC).

## 3.3 Materials

### *3.3.1 Chemicals*

Methyl 2-bromopropionate (Sigma-Aldrich, 98%) and *tert*-butyl acrylate (Sigma-Aldrich, 98%) were fractionally distilled under reduced pressure and sealed under nitrogen prior to use. Copper (I) bromide (Sigma-Aldrich, 98%) and N-N'-N'-N"-N" pentamethyldiethylenetriamine (Sigma-Aldrich, 97%) were used as received. Trifluoroacetic acid (Alfa Aesar, 98%) was used as received. Poly(ethylene oxide) (Sigma-Aldrich, $M_n \sim 2,000$ g mol$^{-1}$, from $^{1}$H NMR) was dried at 40 °C under reduced

pressure for 24 h prior to use. Pluronic P85™ (BASF, $M_n$ ~ 4,600 g $mol^{-1}$, from SEC) was dried at 50 °C under reduced pressure for 24 h prior to use. Propylene oxide (Sigma-Aldrich, 98%) and ethylene oxide (Sigma-Aldrich, 99%) were used as received. 1,12-Dodecanediol (Sigma-Aldrich) was used as received. IMPACT catalyst ($Zn_3[Co(CN)_6]_2$, kindly donated by Bayer Material Science) was dried under vacuum at room temperature for 24 h prior to use. Triethylamine (Sigma-Aldrich, 99%) and 2-bromoisobutyryl bromide (Sigma-Aldrich, 98%) were used as received.

*3.3.2 Solvents*

Toluene (Fisher, HPLC Grade) was deoxygenated for 1 h under a nitrogen sparge. Tetrahydrofuran (Fisher HPLC Grade) was dried and distilled from sodium and benzophenone under a nitrogen atmosphere prior to use. Hexane, dichloromethane, chloroform, diethyl ether, acetone and methanol (all HPLC Grade from Fisher Scientific) were used as received.

**3.4 Characterization**

All $^1H$ NMR spectra were obtained on a Varian Unity 400 NMR spectrometer operating at 400 MHz. The NMR parameters included a pulse width of 28.6° and a relaxation delay of 1.000 sec at ambient temperature. The samples were dissolved in either *d*-$CHCl_3$ or $d_6$-DMSO for obtaining the spectra. Molecular weights and molecular weight distributions of the polyethers and polyacrylates were measured by size exclusion chromatography (SEC) in HPLC grade chloroform at 30 °C on a Waters Alliance Model 2690 chromatograph equipped with a Waters HR 0.5 + HR 2 + HR 3 + HR 4 styragel column set. A Viscotek T60A viscosity detector and a refractive index detector were utilized with polystyrene calibration standards to generate a universal molecular weight

calibration curve for absolute molecular weight analyses. Samples were prepared by dissolving 15-20 mg in 10 mL of HPLC grade chloroform.

### 3.5 Synthesis of Poly(*tert*-butyl acrylate) Homopolymers

#### *3.5.1 Synthesis of Poly(*tert-*butyl acrylate) in Acetone*

The following procedure for ATRP polymerization was adapted from Matyjaszewski et al.[79] A 100-mL schlenk flask was equipped with a stir bar and septum and flame dried under a nitrogen purge prior to use. Cu(I)Br (0.191 g, 1.33 x $10^{-3}$ mol) was charged to the flask and dissolved in 5 mL of acetone. The solution was stirred and subjected to a freeze-thaw technique to remove oxygen. The flask was placed in liquid nitrogen until the reaction mixture had frozen. Once frozen, the flask was removed from the liquid nitrogen and vacuum was applied. Vacuum was applied until the pressure gauge read 1 millitorr. The vacuum was removed and the solution was allowed to warm to room temperature via a warm water bath. The flask was then back-filled with nitrogen gas. This freeze-thawing process was repeated three times.

*Tert*-butyl acrylate (4 g, 3.12 x $10^{-2}$ mol) was charged to the reaction flask and the mixture was stirred and freeze-thawed once. Methyl 2-bromopropionate (0.22 g, 1.33 x $10^{-3}$ mol) was charged to the flask and the solution was stirred and freeze-thawed once. Finally, PMDETA (0.23 g, 1.33 x $10^{-3}$ mol) was charged to the flask and reaction mixture turned from a clear and colorless solution to a light green. This signified formation of the ligand/copper complex from Cu(I)Br and PMDETA. The solution was freeze-thawed twice, then was heated to 60 °C and reacted for 12 h. The reaction was cooled to room temperature. The solution was dissolved in 200 mL of dichloromethane and passed through a neutral alumina column twice to remove the copper/ligand complex. The

dichloromethane was removed via rotary evaporation at 30 °C. The poly(*tert*-butyl acrylate) (P*t*BA) was dried under reduced pressure at 40 °C for 24 h. P*t*BA was a solid with a slight yellow tint. $^{1}$H NMR showed that the reaction had proceeded to 90% conversion and $M_N$ was calculated to be 2,100 g mol$^{-1}$ based on the ratio of repeat units to initiator. SEC supported the $^{1}$H NMR data with a $M_N$ of 2,900 g mol$^{-1}$ and a PDI of 1.10.

*3.5.2 Synthesis of Poly(*tert-*butyl acrylate) in Toluene*

The above procedure was replicated to polymerize *tert*-butyl acrylate in toluene. In brief, a 100-mL schlenk flask was equipped with a stir bar and flame dried under a nitrogen purge. Cu(I)Br (0.115 g, 8.0 x 10$^{-4}$ mol) was charged to the flask and dissolved in 3 mL of deoxygenated toluene. The solution was freeze-thawed three times. *Tert*-butyl acrylate (4 g, 3.12 x 10$^{-2}$ mol) was charged to the reaction flask and the mixture was stirred and freeze-thawed once. Methyl 2-bromopropionate (0.134 g, 8.0 x 10$^{-4}$ mol) was charged to the flask and the solution was stirred and freeze-thawed once. Finally, PMDETA (0.138 g, 8.0 x 10$^{-4}$ mol) was charged to the flask and freeze-thawed twice more and the reaction was heated to 80 °C and reacted for 12 h. The same purification method was utilized as described above. P*t*BA was dissolved in 200 mL of dichloromethane and passed through a neutral alumina column twice. The dichloromethane was removed via a rotary evaporator and dried overnight under reduced pressure at 40 °C. $^{1}$H NMR showed 65% conversion and $M_N$ calculated on the basis of the number of repeat units per initiator was 3,300 g mol$^{-1}$. SEC showed a $M_N$ of 3,900 g mol$^{-1}$ with a PDI of 1.15.

**3.6 Synthesis of Poly(ethylene oxide-*b*-propylene oxide-*b*-ethylene oxide)**

*3.6.1 Synthesis of Poly(propylene oxide) Initiated by 1,12-Dodecanediol*

In a 50-mL round-bottom flask equipped with a stir bar, the heterogeneous $Zn_3[Co(CN)_6]_2$ IMPACT catalyst (0.0011 g) was dispersed in 2 mL of distilled THF. 1,12-Dodecanediol (0.64 g, 3.12 x $10^{-3}$ mol) was charged to the flask and the initiator solution was stirred for 24 h to let the diol adsorb onto the catalyst. Propylene oxide (8.29 mL, 0.143 mol) was charged into a stainless steel high pressure 300-mL Parr reactor, then 5 mL of THF was added and the vessel was pressurized to 30 psi with nitrogen gas. The initiator solution was charged to the reactor followed by 5 mL THF. The reaction mixture was heated to 100 °C. The pressure increased from 30 psi at room temperature to 140 psi at 100 °C. A tremendous increase in pressure occurred almost immediately once the reaction temperature had reached 100 °C, 140 psi to 200 psi. The reaction was allowed to progress until the pressure spike subsided and returned to approximately 140 psi. The reaction mixture was cooled to room temperature, dichloromethane was added (100 mL), and the mixture was passed through a neutral celite column twice to remove the catalyst. The dichloromethane was removed via rotary evaporation and the PPO was dried overnight at 40 °C under reduced pressure. $^1$H NMR confirmed a $M_N$ of 3,400 g $mol^{-1}$.

*3.6.2 Preparation of Potassium Naphthalide Solution*

Potassium naphthalide solution in THF was prepared by the method of Thompson et al.[80] A representative procedure to prepare a 0.96 M solution of potassium naphthalide in THF is provided. Naphthalene (0.095 mol, 12.16 g) was weighed into a 250-mL flame dried round-bottom flask equipped with a glass coated magnetic stir bar, sealed with a septum, and purged with nitrogen. THF (100 mL) was transferred to the flask via a glass

syringe. Potassium (0.095 mol, 3.7 g) was cut, the packing oil was removed by blotting on a Kimwipe, and quickly added to the flask. The flask was resealed and purged with nitrogen. The reaction flask was covered with aluminum foil and the mixture was stirred for 24 h to form a dark green liquid. It was titrated against a standardized HCl solution to obtain the exact concentration.

*3.6.3 Synthesis of Poly(ethylene oxide-b-propylene oxide-b-ethylene oxide)*

The synthesis of the triblock polyether follows a similar procedure as explained above for synthesis of PPO except that potassium alkoxide was the propagating species. In a 50-mL round-bottom flask equipped with a stir bar, PPO (8 g, 2.4 x $10^{-3}$ mol) was dissolved in 5 mL THF followed by potassium naphthalide solution (2.45 mL, 2.4 x $10^{-3}$ mol). The macroinitiator solution was stirred for one hour prior to use. The Parr reactor was cooled to -40 °C using a dry ice bath and ethylene oxide (5 g, 0.114 mol) was distilled into the reactor, then 5 mL of THF was added and the mixture was pressurized to 30 psi with nitrogen gas. The macroinitiator solution was then charged to the reactor followed by 5 mL THF. The dry ice bath was removed and the solution was allowed to warm to room temperature and react for 24 h. The reaction was terminated using a 2.5 M solution of acetic acid (0.94 mL, 2.4 x $10^{-3}$ mol) to protonate the polyether alkoxide termini. The polyether triblock was concentrated by removing THF via the rotary evaporator. This solution was precipitated into a 50:50 hexane/diethyl ether mixture (400 mL, 200 mL each). The yellow precipitate was vacuum filtered, collected, and dried at 40 °C under reduced pressure for 24 h. $^{1}$H NMR showed a $M_N$ of 1,300 g mol$^{-1}$ for each PEO segment, with a total $M_n$ of 6,400 g mol$^{-1}$ for HO-PEO-PPO-PEO-OH. SEC showed a $M_n$ of 4,900 g mol$^{-1}$ with a PDI of 1.31.

### 3.7 Synthesis of Polyether-polyacrylate Block Copolymers

*3.7.1 Bromination of HO-PEO-PPO-PEO-OH*

In a 250-mL flame-dried round-bottom flask equipped with a stir bar, HO-PEO-PPO-PEO-OH (7.6 g, 1.19 x $10^{-3}$ mol) was dissolved in 100 mL of freshly-distilled THF. Triethylamine (0.289 g, 2.86 x $10^{-3}$ mol) was charged to the flask and the solution was stirred and cooled to 0 °C using an ice water bath. 2-Bromoisobutyryl bromide (0.602 g, 2.62 x $10^{-3}$ mol) was charged to the reaction flask and the solution was stirred for 20 min. Immediately, white salts began to form indicating reaction progression. The water bath was removed and the reaction was stirred for 24 h.

The triethylammonium bromide salts were removed via gravity filtration and the THF was removed via rotary evaporation. Br-PEO-PPO-PEO-Br was re-dissolved in dichloromethane and washed with DI water twice. The organic layer was collected and the polymer was concentrated in dichloromethane via rotary evaporation. The polymer was precipitated into a 50:50 hexane/ether mixture (400 mL, 200 mL each) to remove any excess amine. The slight yellow precipitate was collected and dried under reduced pressure at 40 °C for 24 h.

*3.7.2 Synthesis of Poly(*tert-*butyl acrylate-b-ethylene oxide-b-propylene oxide-b-ethylene oxide-b-*tert-*butyl acrylate)*

The polyether-poly(*tert*-butyl acrylate) pentablock copolymer was polymerized via ATRP. In a 100-mL flame-dried schlenk flask equipped with a stir bar, Br-PEO-PPO-PEO-Br (1.3 g, 2.23 x $10^{-4}$ mol) was dissolved in 4 mL of deoxygenated toluene. The solution was freeze-thawed three times. *Tert*-butyl acrylate (2.0 g, 1.56 x $10^{-2}$ mol) was charged to the flask and the solution was freeze-thawed followed by the addition of PMDETA (0.08 g, 4.46 x $10^{-4}$ mol). The solution was freeze-thawed once more before

the addition of Cu(I)Br. The schlenk flask was opened under a nitrogen purge and Cu(I)Br (0.064 g, 4.46 x $10^{-4}$ mol) was charged to the flask. The solution was resealed with a septum and was freeze-thawed twice more. The reaction was allowed to proceed for 12 h at 80 °C.

The polyether-poly(*tert*-butyl acrylate) pentablock copolymer was purified by dissolving the reaction mixture in 100 mL of dichloromethane and the solution was passed through a neutral alumina column twice. The dichloromethane was removed via rotary evaporation. The pentablock copolymer was dried at 40 °C overnight under reduced pressure. The resulting viscous liquid product, PtBA-PEO-PPO-PEO-PtBA, was clear with a slight yellow tint. The excess monomer was removed during subsequent removal of the *tert*-butyl group. $^{1}$H NMR showed 77% conversion of monomer with a combined $M_n$ of the PtBA blocks of 6,800 g $mol^{-1}$. The total $M_n$ determined of the pentablock determined by $^{1}$H NMR was 12,800 g $mol^{-1}$. SEC showed a total $M_n$ of 22,000 g $mol^{-1}$ with a PDI of 1.17.

*3.7.3 Bromination of Pluronic P85™, HO-$PEO_{26}$-$PPO_{41}$-$PEO_{26}$-OH*

In a 250-mL flame-dried round-bottom flask equipped with a stir bar, HO-$PEO_{26}$-$PPO_{41}$-$PEO_{26}$-OH, Pluronic P85™, (10.16 g, 2.20 x $10^{-3}$ mol) was dissolved in 100 mL of distilled THF. Triethylamine (0.534 g, 5.28 x $10^{-3}$ mol) was charged to the flask and the solution was stirred and cooled to 0 °C using an ice water bath. 2-Bromoisobutyryl bromide (1.11 g, 4.84 x $10^{-3}$ mol) was charged to the reaction flask and the solution was stirred for 20 min. Immediately, white salts began to form indicating progression. The water bath was removed and the reaction was allowed to proceed for 24 h.

The triethylammonium bromide salts were removed via gravity filtration and the THF was removed via rotary evaporation. Br-$PEO_{26}$-$PPO_{41}$-$PEO_{26}$-Br was re-dissolved in dichloromethane (100 mL) and washed with DI water twice. The organic layer was collected and the polymer was concentrated in dichloromethane via rotary evaporation and the polymer was precipitated into a 50:50 hexane/ether to remove any excess amine. The white precipitate was collected and dried under reduced pressure at 40 °C for 24 h.

*3.7.4 Synthesis of $PtBA_{27}$-$PEO_{26}$-$PPO_{41}$-$PEO_{26}$-$PtBA_{27}$*

The synthesis the polyether-poly(*tert*-butyl acrylate) block copolymer was derived from the brominated Pluronic P85™, Br-$PEO_{26}$-$PPO_{41}$-$PEO_{26}$-Br. In a 100-mL flame-dried schlenk flask equipped with a stir bar, Br-$PEO_{26}$-$PPO_{41}$-$PEO_{26}$-Br (2.0 g, 4.08 x $10^{-4}$ mol) was dissolved in 4 mL of deoxygenated toluene. The solution was freeze-thawed three times. *Tert*-butyl acrylate (3.65 g, 2.85 x $10^{-2}$ mol) was charged to the flask and the solution was freeze-thawed followed by the addition of PMDETA (0.071 g, 4.08 x $10^{-4}$ mol). The solution was freeze-thawed once more before the addition of Cu(I)Br. The schlenk flask was opened under a nitrogen purge, and Cu(I)Br (0.058 g, 4.08 x $10^{-4}$ mol) was charged to the flask. The solution was resealed with a septum and was freeze-thawed twice more. The reaction was allowed to proceed for 12 h at 80 °C.

The PtBA-$PEO_{26}$-$PPO_{41}$-$PEO_{26}$-PtBA was dissolved in 100 mL of dichloromethane and the solution was passed through a neutral alumina column twice to remove the copper/ligand complex. The dichloromethane was removed via rotary evaporation. PtBA-$PEO_{26}$-$PPO_{41}$-$PEO_{26}$-PtBA was dried at 40 °C overnight under reduced pressure. The resulting product, PtBA-$PEO_{26}$-$PPO_{41}$-$PEO_{26}$-PtBA was clear with a slight yellow tint. The excess monomer was removed during hydrolysis of the

*tert*-butyl group. $^{1}$H NMR showed 78% conversion of monomer with a combined $M_n$ of the PtBA blocks of 6,900 g mol$^{-1}$. The total $M_n$ determined of the pentablock determined by $^{1}$H NMR was 11,800 g mol$^{-1}$. SEC showed a total $M_n$ of 24,000 g mol$^{-1}$ with a PDI of 1.15.

*3.7.5 Deprotection of $PtBA_{27}$-$PEO_{26}$-$PPO_{41}$-$PEO_{26}$-$PtBA_{27}$*

In a 250-mL round-bottom flask, $PtBA_{27}$-$PEO_{26}$-$PPO_{41}$-$PEO_{26}$-$PtBA_{27}$ (2.0 g, 1.57 x $10^{-4}$ mol based on $^{1}$H NMR, 9.45 x $10^{-3}$ mol *t*-butyl groups) was dissolved in 70 mL of dichloromethane. Trifluoroacetic acid (10.77 g, 9.45 x $10^{-2}$ mol) was charged to the flask with a 10:1 mole ratio of acid to *t*-butyl groups. The solution was stirred at room temperature for 24 h.

During deprotection, the polyether-polyacrylate gels and precipitates out of solution due to the tendency of the carboxylic acid protons to hydrogen bond to the oxygens of PEO.[81] The deprotected pentablock, $PAA_{27}$-$PEO_{26}$-$PPO_{41}$-$PEO_{26}$-$PAA_{27}$, was concentrated by removing the dichloromethane via rotary evaporation. The pentablock copolymer was re-dissolved in 10 mL THF and placed in a 1,000 g mol$^{-1}$ MWCO cellulose acetate dialysis bag to remove excess monomer and acid. The solution was dialyzed against 4 L of deionized water for 48 h, changing the DI water each day. As the THF is displaced by DI water, the polymer begins to precipitate from the solution. The pentablock was then freeze-dried for 48 h to remove the DI water. $^{1}$H NMR showed complete hydrolysis of all *tert*-butyl groups.

*3.7.6 Bromination of 2,000 g mol$^{-1}$ $CH_3$-PEO-OH*

In a 250-mL flame-dried round-bottom flask equipped with a stir bar, $CH_3O$-$PEO_{45}$-OH (10.06 g, 5.03 x $10^{-3}$ mol) was dissolved in 100 mL of distilled THF.

Triethylamine (0.611 g, 6.04 x $10^{-3}$ mol) was charged to the flask and the solution was stirred and cooled to 0 °C using an ice water bath. 2-Bromoisobutyryl bromide (1.27 g, 5.53 x $10^{-3}$ mol) was charged to the reaction flask and the solution was stirred for 20 min. White salts began to precipitate immediately. The water bath was removed and the reaction was allowed to proceed for 24 h.

The triethylammonium bromide salts were removed via gravity filtration and the THF was removed via rotary evaporation. $CH_3O$-$PEO_{45}$-Br was re-dissolved in dichloromethane (100 mL) and washed with DI water twice. The dichloromethane was removed via rotary evaporation and the polymer was precipitated into a 50:50 hexane/ether mixture to remove any excess amine. The white precipitate was collected and dried under reduced pressure at 40 °C for 24 h.

*3.7.7 Synthesis of a Poly(ethylene oxide)-b-poly(*tert-*butyl acrylate) Diblock Copolymer*

The synthesis of a polyether-poly(*tert*-butyl acrylate) diblock copolymer follows a similar synthetic scheme and as described above. Briefly, a 2,150 g $mol^{-1}$ $CH_3O$-PEO-Br (2.0 g, 9.30 x $10^{-4}$ mol) oligomer was dissolved in 4 mL of deoxygenated toluene in a 100-mL flame-dried schlenk flask equipped with a stir bar. The solution was freeze-thawed three times. *Tert*-butyl acrylate (17.86 g, 0.139 mol) was charged to the flask and the solution was freeze-thawed once. PMDETA (0.161, 9.30 x $10^{-4}$ mol) was charged to the flask and the solution was freeze-thawed once more. Finally, Cu(I)Br (0.133 g, 9.30 x $10^{-4}$ mol) was charged to the flask and the solution was freeze-thawed two more times. The reaction was allowed to proceed for 12 h at 80 °C.

The $CH_3O$-$PEO_{45}$-PtBA was purified by dissolving the reaction mixture in 100 mL of dichloromethane and the solution was passed through a neutral alumina column

twice to remove the copper/ligand complex. The dichloromethane was removed via rotary evaporation. $CH_3O$-$PEO_{45}$-PtBA was dried at 40 °C overnight under reduced pressure. The resulting product, $CH_3O$-$PEO_{45}$-PtBA was clear with a slight yellow tint. The excess monomer was removed during the hydrolysis of the *tert*-butyl group. $^1$H NMR showed 78% conversion of monomer with a $M_n$ of the PtBA block of 15,000 g mol$^{-1}$. The total $M_n$ determined of the diblock determined by $^1$H NMR was 17,000 g mol$^{-1}$. SEC showed a total $M_n$ of 23,000 g mol$^{-1}$ with a PDI of 1.18.

*3.7.8 Deprotection of $CH_3O$-$PEO_{45}$-$PtBA_{117}$*

$CH_3O$-$PEO_{45}$-$PtBA_{117}$ was deprotected following a similar procedure as previously described. In a 250-mL round-bottom flask equipped with a stir bar, $CH_3O$-$PEO_{45}$-$PtBA_{117}$ (2.0 g, 1.67 x 10$^{-4}$ mol, 1.36 x 10$^{-2}$ mol *t*-butyl groups) was dissolved in 80 mL of dichloromethane. Trifluoroacetic acid (15.56 g, 1.36 x 10$^{-1}$ mol) was charged to the flask with a 10:1 mole ratio of acid to *t*-butyl groups. The solution was stirred at room temperature for 24 h. During deprotection, the polyether-polyacrylate diblock gels and precipitates from solution due to the tendency of the carboxylic acid protons to hydrogen bond to the oxygens of PEO.[81]

The deprotected diblock, $CH_3O$-$PEO_{45}$-$PAA_{117}$, was concentrated by removing the dichloromethane via rotary evaporation. The copolymer was re-dissolved in 10 mL of THF and placed in a 1,000 g mol$^{-1}$ MWCO cellulose acetate dialysis bag to remove excess monomer and acid. The solution was dialyzed against 4 L of DI water for 48 h, changing the DI water each day. As the THF is displaced by DI water, the polymer begins to precipitate. The diblock was freeze-dried for 48 h to remove the DI water. $^1$H NMR showed complete hydrolysis of all *tert*-butyl groups.

## 3.8 Results and Discussion

### *3.8.1 Homopolymeriztion of tert-butyl acrylate*

The polymerization of *tert*-butyl acrylate was investigated in acetone and toluene as solvents. Methyl 2-bromopropionate was utilized as the initiator. During the reaction, Cu(I)Br oxidizes to Cu(II)Br yielding a secondary radical on the initiator. This radical is then free to react with *tert*-butyl acrylate. Figure 3.3 shows a representative $^{1}$H NMR spectrum of the methyl 2-bromopropionate initiator. Each integration value corresponds well with the theoretical number of protons in each chemical environment.

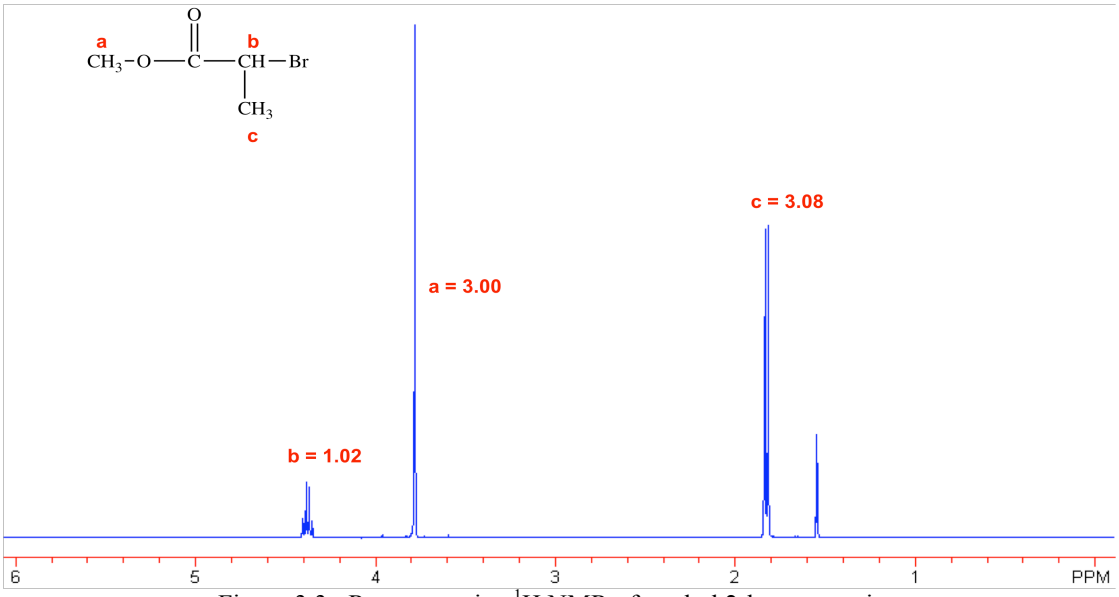


Figure 3.3: Representative $^{1}$H NMR of methyl 2-bromopropionate

Figure 3.4 shows $^{1}$H NMR homopolymer spectra. The target molecular weights at full monomer conversion were 2,300 and 5,000 g mol$^{-1}$ for PtBA reactions in acetone and toluene respectively. As seen in figure 3.4 for the polymer prepared in acetone, applying an integration value of 3.00 for the methyl ester protons yields an integration value of 16.38 for the methine peak from the PtBA backbone at 2.2 ppm. From this methine proton peak the molecular weight of the homopolymer can be calculated. As for the

polymerization performed in toluene, the methine peak at 2.2 ppm equals 24.89, which corresponds to 3,300 g $mol^{-1}$ and a 65% conversion of monomer.

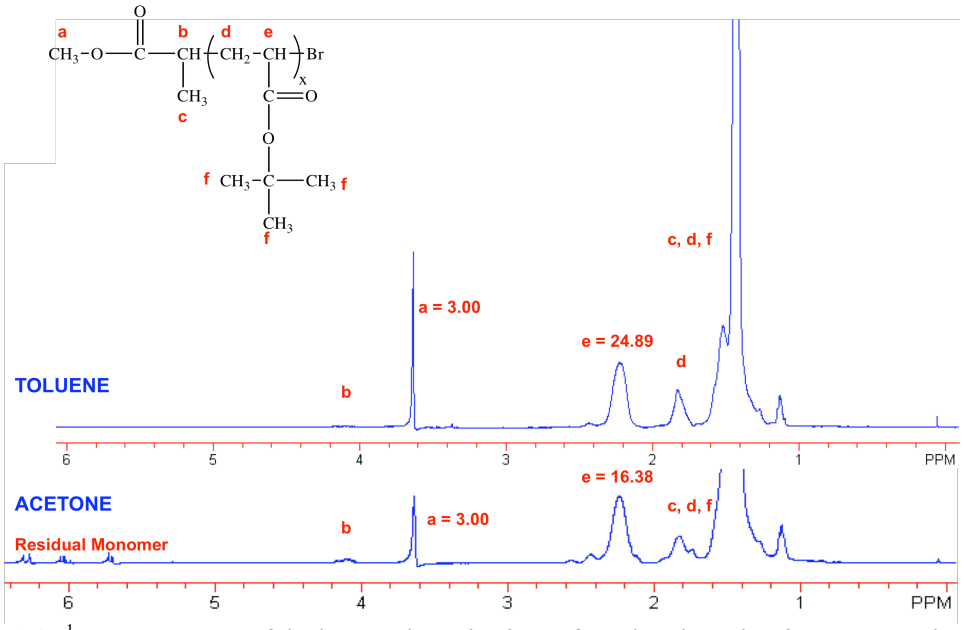


Figure 3.4: $^{1}$H NMR spectra of the homopolymerizations of *tert*-butyl acrylate in acetone and toluene

The *tert*-butyl acrylate homopolymer reactions were relatively controlled (table 3.1). In each case, the SEC $M_n$, however, was larger than that calculated from the NMR spectra by assuming one initiator residue per chain. This may be attributable to a small amount of termination by combination. This trend was even more pronounced when using difunctional brominated polyether triblocks as macroinitiators (table 3.2).

| Solvent | Target $M_n$ (g $mol^{-1}$) | GPC $M_n$ (g $mol^{-1}$) | PDI |
|---|---|---|---|
| Acetone | 2,100 | 2,900 | 1.11 |
| Toluene | 3,300 | 4,100 | 1.13 |

Table 3.1: Summary homopolymerization data of *tert*-butyl acrylate in acetone and toluene

*3.8.2 Synthesis of polyether triblock copolymers (HO-PEO-PPO-PEO-OH)*

The polymerization of PO was initiated with 1,12-dodecanediol (figure 3.5). The $^{1}$H NMR spectrum shows four peaks corresponding to the four different chemical

environments of 1,12-dodecanediol. The polymerization of PO was conducted with the zinc hexacyanocobaltate (IMPACT) heterogeneous catalyst. During the reaction, the zinc binds to hydroxyl groups and catalyzes ring-opening polymerizations of epoxides and other monomers.[82] In the presence of a smaller diol such as 1,3-propanediol, the diol and catalyst have been reported to form a stable five or six membered ring, and this greatly inhibits the desired polymerizations.[82] Typically, the polymerization of PO using the zinc hexacyanocobaltate catalyst proceeds very rapidly and is accompanied by a sharp exotherm with a corresponding increase in pressure. Attempts to prepare PPO with this coordination catalyst and 1,3-propanediol as the initiator were unsuccessful.

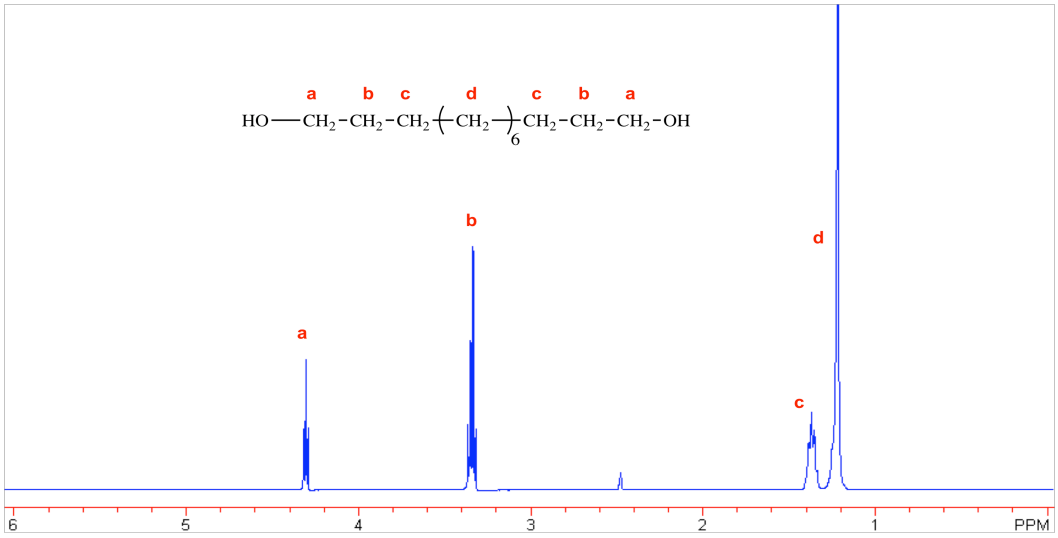

Figure 3.5: 1H NMR of 1,12-dodecandiol, initiator of PO.

The ring-opening of PO initiated with 1,12-dodecanediol and catalyzed by $Zn_3[Co(CN)_6]_2$ was conducted in a Parr pressure reactor at 110 °C and 150 psi. Under these conditions, well-defined PPO was produced that was free from the allyl endgroups that form in side reactions utilizing alkoxides as the propagating species. The methyl protons pendent on the PO monomer are acidic. Under basic conditions, a side reaction occurs in which a methyl proton is removed leading to the formation of an unsaturated

initiator. This unsaturated initiator is free to polymerize any unreacted PO rings. $^{1}$H NMR, figure 3.6 (a), shows the results of the polymerization of PO utilizing the coordination catalyst. The two initiator peaks appear at 1.2 and 1.6 ppm. The methyl peak of the PPO polymer appears at 1.1 ppm. Additionally, the methylene and methine protons appear around 3.5 ppm. The resulting $M_n$ of PPO was 3,200 g mol$^{-1}$. No allyl protons were present between 5-6 ppm, which would be indicative of any unsaturated PPO homopolymers.

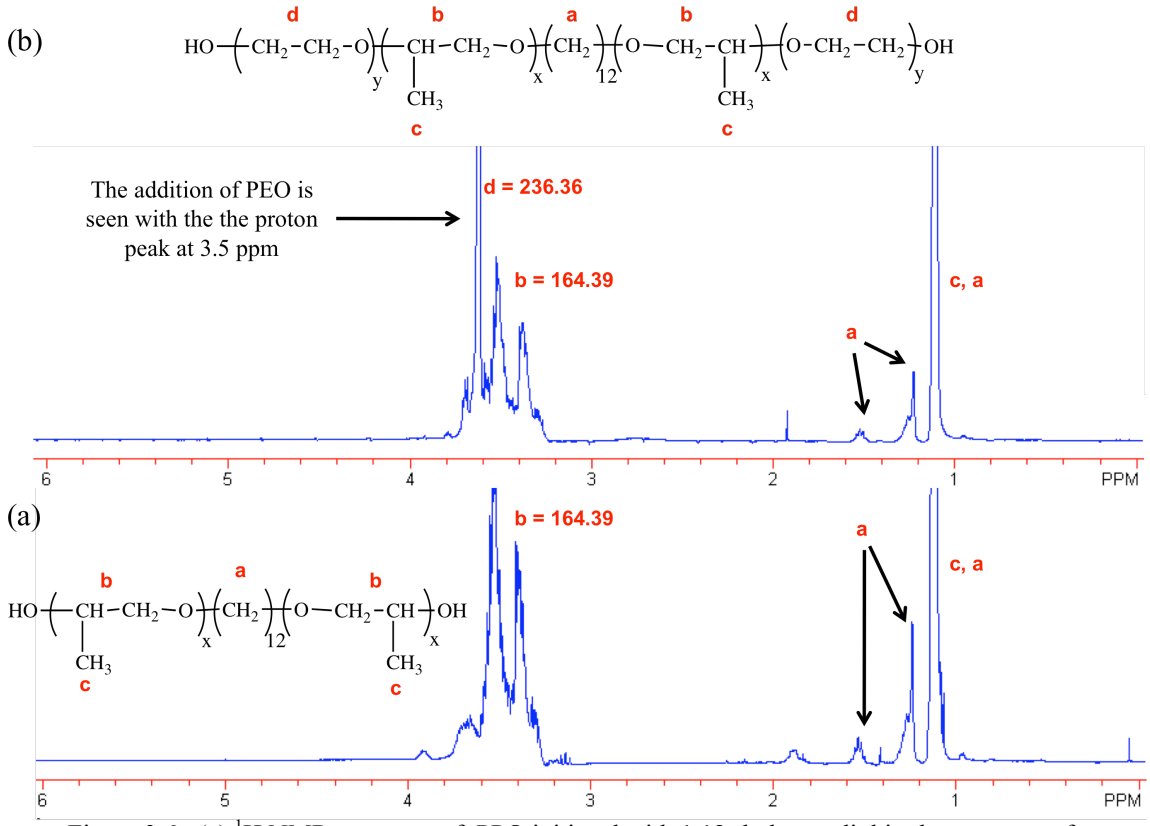


Figure 3.6: (a) $^{1}$H NMR spectrum of PPO initiated with 1,12-dodecanediol in the presence of $Zn_3[Co(CN)_6]_2$, and (b) the macroinitiation of EO with PPO catalyzed by base

The 3,200 g mol$^{-1}$ PPO was utilized in a subsequent reaction to initiate EO in basic conditions. Figure 3.6(b) shows that the PPO macroinitiator was successfully utilized to polymerize EO. The polymer peak that appears at 3.6-3.7 ppm is a direct

representation of the methylene protons associated with the PEO backbone. The combined PEO $M_n$ was calculated to be 2,600 g $mol^{-1}$. $^1H$ NMR showed a total $M_n$ of 5,800 g $mol^{-1}$ and SEC confirmed a total $M_n$ of 6,500 g $mol^{-1}$ with a PDI of 1.07.

*3.8.3 Formation of a brominated macroinitiator for ATRP - Br-PEO-PPO-PEO-Br*

The hydroxyl functionalities on the termini of the polyether triblock copolymer were reacted with 2-bromoisobutyryl bromide to yield a tertiary bromide group at each terminus of the triblock copolymer. Figure 3.7 shows a representative $^1H$ NMR spectrum of Br-PEO-PPO-PEO-Br. The sharp singlet at 2.0 ppm indicates the successful addition of 2-bromoisobutyryl bromide.

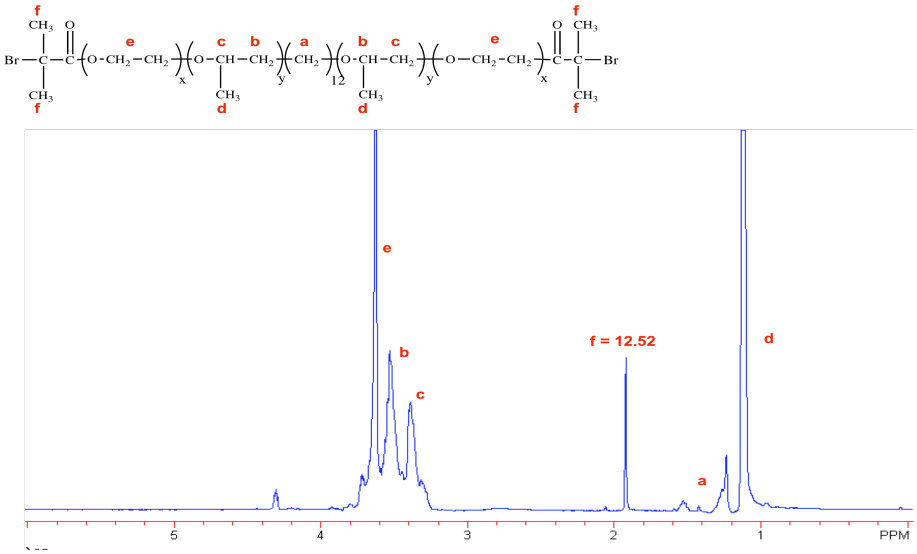


Figure 3.7: Bromination of HO-PEO-PPO-PEO-OH utilizing 2-bromoisobutyryl bromide

*3.8.4 Synthesis of pentablock copolymers by ATRP - PtBA-PEO-PPO-PEO-PtBA*

Br-PEO-PPO-PEO-Br was utilized as a macroinitiator for polymerization of *tert*-butyl acrylate by atom transfer free radical polymerization. Cu(I)Br is oxidized during the reaction to form Cu(II)$Br_2$ producing a tertiary radical on the polymer termini. The $^1H$ NMR spectrum shown in figure 3.8 confirms the polymerization of *tert*-butyl acrylate. The peaks at 1.2-1-4, 1.8, and 2.2 ppm represent the methyl, methylene, and methine

protons respectively of the poly(*tert*-butyl acrylate) backbone. The methine peak at 2.2 ppm was utilized to determine the molecular weights of the PtBA blocks, 3,400 g $mol^{-1}$. SEC results indicated a total molecular weight of 22,000 g $mol^{-1}$ and a PDI of 1.17. Figure 3.9 shows a representative SEC trace of HO-PEO-PPO-PEO-OH. The living polymerization of PO and EO yields a narrow molecular weight polyether triblock. However, the subsequent polymerization of *tert*-butyl acrylate using Br-PEO-PPO-PEO-Br yields polymers with somewhat broader distributions. The $M_N$s that were calculated from the $^1$H NMR and SEC data differ, and this can likely be attributed to some chain coupling during the ATRP process.

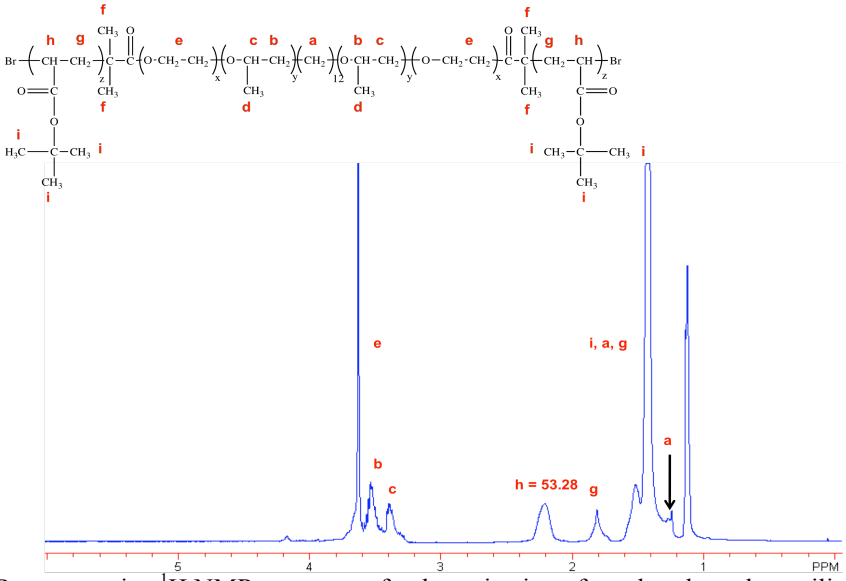


Figure 3.8: Representative $^1$H NMR spectrum of polymerization of *tert*-butyl acrylate utilizing Br-PEO-PPO-PEO-Br as a macroinitiator


Figure 3.9: SEC trace of the precursor, HO-PEO-PPO-PEO-OH. A narrow molecular weight distribution is noticed indicative of living polymerizations. No low molecular weight shoulder occurs due to initiation of PPO with allylfunctional groups

### *3.8.5 Polyether Macroinitiators for ATRP -Br-$PEO_{26}$-$PPO_{41}$-$PEO_{26}$-Br*

A Pluronic P85™ polyether triblock copolymer was brominated using 2-bromoisobutyryl bromide for comparison. Figure 3.10 shows a representative $^{1}$H NMR spectrum of a brominated P85 polyether. The presence of a sharp singlet at 2.0 ppm is indicative of the methyl protons from 2-bromoisobutryyl bromide.

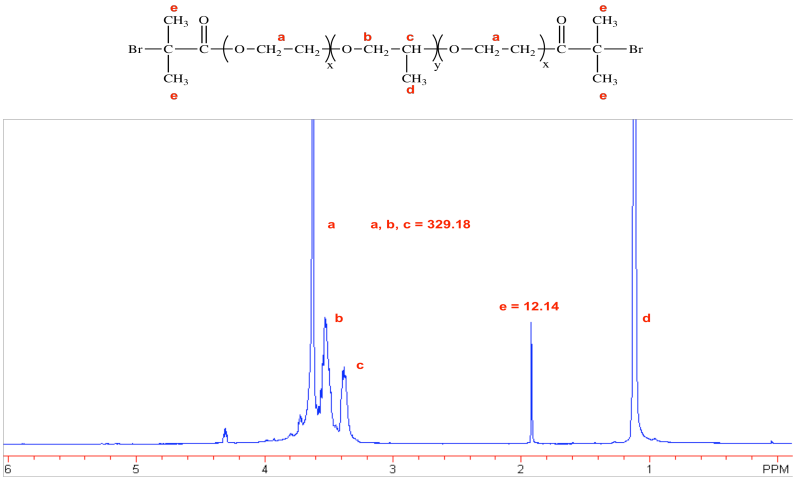


Figure 3.10: $^{1}$H NMR spectrum of a brominated 4,600 g mol$^{-1}$ Pluronic P85 polyether

### *3.8.6 Results and Discussion of $PtBA_{27}$-$PEO_{26}$-$PP41_{7}$-$PEO_{26}$-$PtBA_{27}$*

The brominated P85 polyether was utilized as a macroinitiator for atom transfer free radical polymerization of *tert*-butyl acrylate. Figure 3.11 shows a representative $^{1}H$ NMR spectrum of the resulting polyether-polyacrylate pentablock.

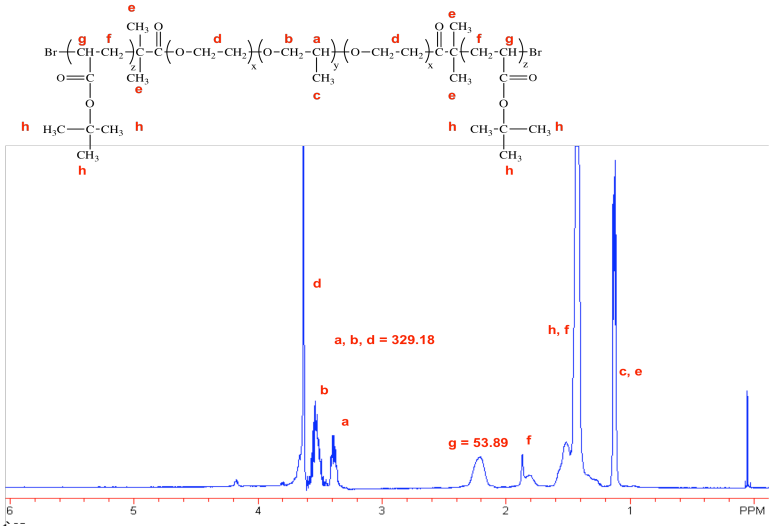


Figure 3.11: $^{1}H$ NMR spectrum of the polymerization of *tert*-butyl acrylate using brominated P85

The methine peak at 2.2 ppm was used to determine the combined molecular weight of PtBA, 6,900 g $mol^{-1}$ with 77 % conversion of PtBA monomer and an overall $M_N$ of 12,000 g $mol^{-1}$. SEC showed a molecular weight of 24,000 g $mol^{-1}$ with a PDI of 1.15. Figure 3.12 shows representative SEC chromatograms of Pluronic P85™ and the corresponding pentablock copolymer that was prepared with the brominated P85 as the initiator. A low molecular weight shoulder is noticed in the trace of Pluronic P85™ due to diblock impurities derived from the allyl-initiated PPO chains. The SEC trace of PtBA-P85-PtBA is narrow and monomodal; however, the ATRP radical polymerization of *tert*-butyl acrylate was not completely controlled. Comparison of the $^{1}H$ NMR data to SEC shows a significant molecular weight discrepancy, which is attributed to chain combination that occurs during the progression of the reaction. The persistent radical was not completely controlled by the Cu(I)Br/ligand complex.

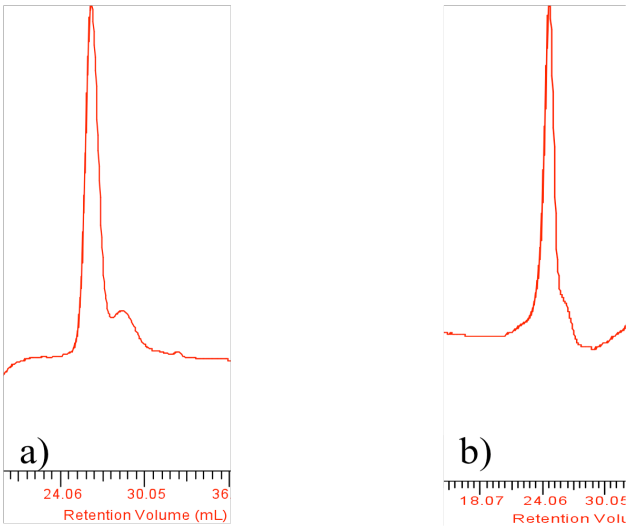

Figure 3.12: GPC traces of a) Pluronic P85 and b) P85-PtBA

*3.8.7 Results and Discussion of $PAA_{27}$-$PEO_{26}$-$PP41_{7}$-$PEO_{26}$-$PAA_{27}$*

The polyether-polyacrylate *tert*-butyl groups were removed by deprotection with trifluoroacetic acid to provide the carboxylic acids required for forming nanoplexes with the antibiotics. The carboxylic acid groups can be deprotonated to produce a negative charge so that they can bind electrostatically to a positively charged drug. Organic conditions were utilized in efforts to avoid any hydrolytic cleavage of the esters that connected the blocks. The block copolymer was deprotected in methylene chloride in the presence of trifluoroacetic acid. As the reaction proceeded, the block copolymer went from being completely soluble in the dichloromethane to becoming a gelled-insoluble material. This phenomenon is due to the hydrogen bonding that occurs between carboxylic acid protons and the oxygens of the PEO.[81] Figure 3.13 shows a representative $^{1}$H NMR spectrum of a deprotected polyether-polyacrylate pentablock. The large polymer peak at 1.5 ppm indicative of the *t*-butyl groups, disappeared indicating removal of the butyl groups.

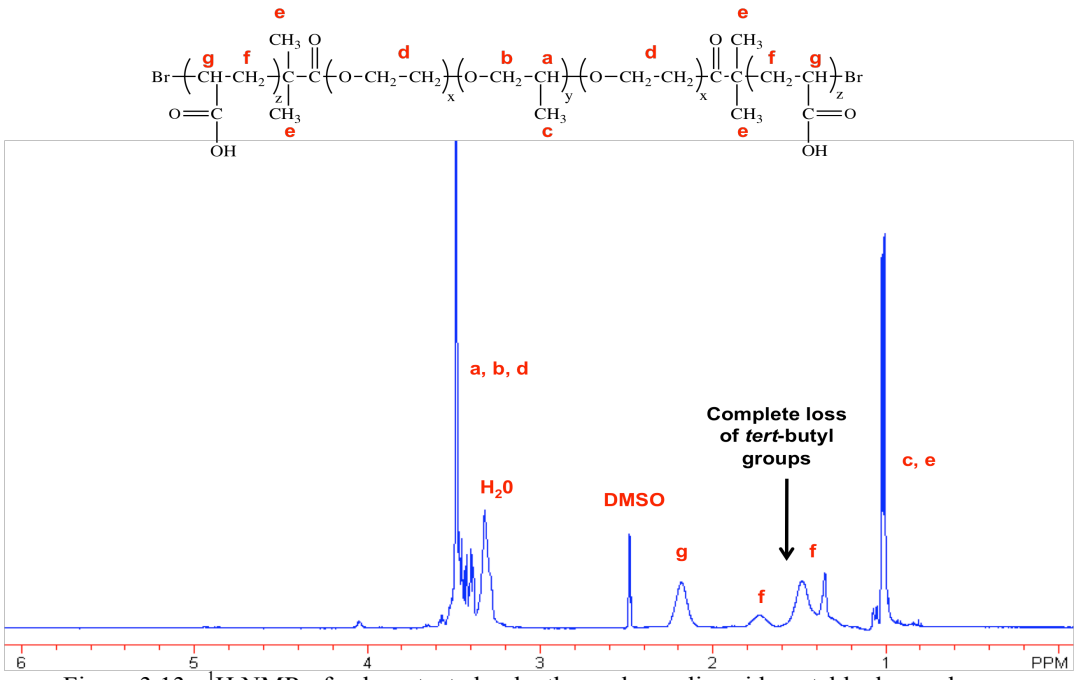

Figure 3.13: $^{1}$H NMR of a deprotected polyether polyacrylic acid pentablock copolymer

*3.8.8 Results and Discussion of $CH_3O$-$PEO_{45}$-Br*

Another block copolymer needed for the polymer-antibiotic nanoplexes was a poly(ethylene oxide-*b*-acrylate) diblock. The PEO aided in steric stabilization of the nanoplexes in aqueous media. The polyacrylate block served to anchor the PEO segment into the nanoplex and also bind to the antibiotic. Following a similar synthetic scheme for the polyether-polyacrylate pentablocks, the diblock was brominated to form the desired macroinitiator. Figure 3.14 shows a representative $^{1}$H NMR spectrum of a 2,000 g mol$^{-1}$ brominated PEO homopolymer. The methyl peak associated with the methyl groups of 2-bromoisobutyryl bromide appears at 2.0 ppm.

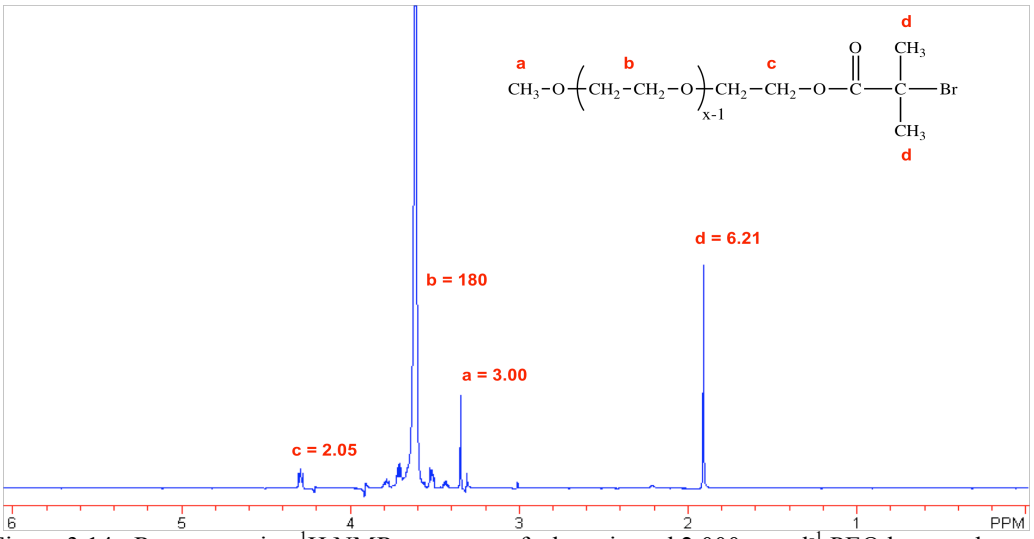

Figure 3.14: Representative $^{1}$H NMR spectrum of a brominated 2,000 g mol$^{-1}$ PEO homopolymer

### *3.8.9 Results and Discussion of $CH_3O$-$PEO_{45}$-$PtBA_{117}$*

The 2,000 g mol$^{-1}$ PEO brominated macroinitiator was utilized to polymerize *t*-butyl acrylate by ATRP. A similar synthetic scheme was followed as for the pentablock copolymers. Figure 3.15 shows a representative $^{1}$H NMR of a 17,000 g mol$^{-1}$ PEO-PtBA diblock copolymer. Again, the methine peak of PtBA appears at 2.2 ppm. A target molecular weight of 19,000 g mol$^{-1}$ PtBA was used in the reaction. The reaction was allowed to progress for 12 hours to yield 78% conversion of monomer. A final molecular weight of 15,000 g mol$^{-1}$ of PtBA was calculated from $^{1}$H NMR. SEC showed a molecular weight of 23,000 g mol$^{-1}$ with a PDI of 1.18. This discrepancy was again attributed to some chain coupling during the ATRP step.

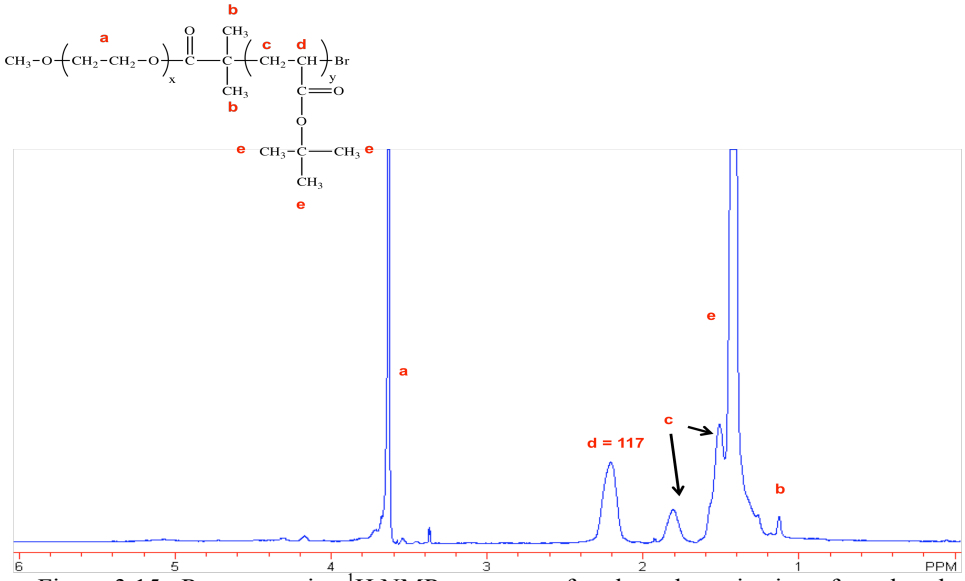


Figure 3.15: Representative $^{1}$H NMR spectrum after the polymerization of *tert*-butyl acrylate using a 2,000 g mol$^{-1}$ PEO homopolymer

### *3.8.10 Results and Discussion of $CH_3O$-$PEO_{45}$-$PAA_{117}$*

Finally, the polyether polyacrylate diblock copolymer was deprotected with trifluoroacetic acid. The reaction proceeded in dichloromethane for 24 hours and the diblock copolymer went from completely soluble to a gelled insoluble polymer due to the tendency of the carboxylic acid protons to hydrogen bond to the oxygens of PEO. Figure 3.16 shows an $^{1}$H NMR spectrum of a deprotected polyether-polyacrylate diblock copolymer. The butyl groups that appeared at 1.2 ppm were completely removed.

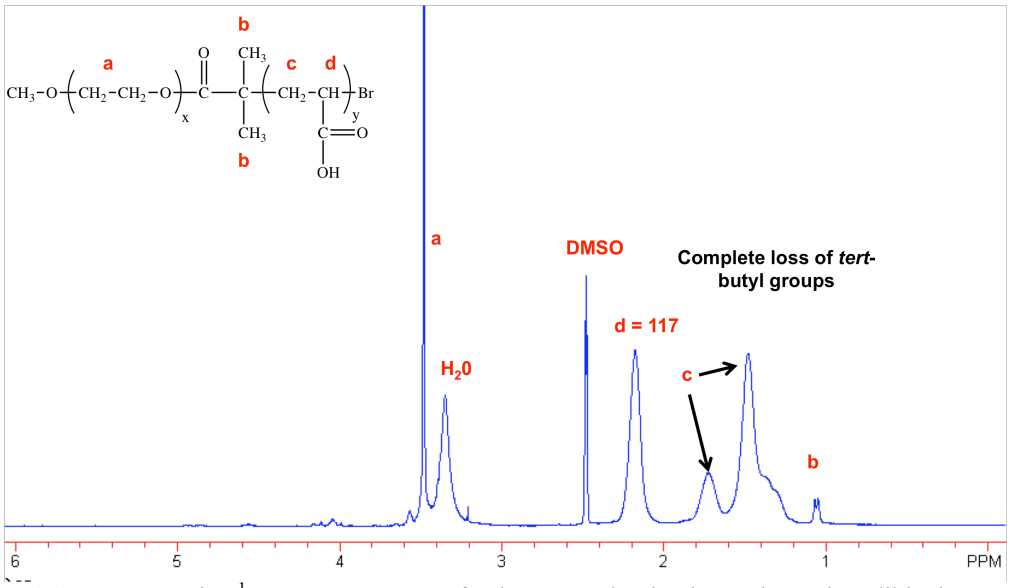

Figure 3.16: Representative $^{1}$H NMR spectrum of a deprotected polyether-polyacrylate diblock copolymer

*3.8.11 Summary of results of polyether-polyacrylate block copolymers*

Several polyether-polyacrylate block copolymers were synthesized (table 3.2). The main discrepancy lies with the distinct difference in molecular weights calculated from the $^{1}$H NMR spectra and SEC chromatograms. $^{1}$H NMR confirmed incorporation of the *t*-butyl acrylate groups into the copolymers. The molecular weights were calculated from this data by taking the precursor molecular weights into consideration and assuming that no side reactions occurred in the ATRP reactions. The discrepancy responsible for the difference between $^{1}$H NMR and SEC might be due to some chain combination that persisted during the polymerization.

| Polymers | Target $M_n$ PtBA (g $mol^{-1}$) | Total $M_n$ (g $mol^{-1}$) | GPC $M_n$ (g $mol^{-1}$) | PDI |
|---|---|---|---|---|
| PtBA (acetone) | 2,100 | - | 2,900 | 1.11 |
| PtBA (toluene) | 3,300 | - | 4,100 | 1.13 |
| PtBA-PEO-PPO-PEO-PtBA | 6,800 | 12,800 | 22,000 | 1.17 |
| PtBA-PEO-PPO-PEO-PtBA (P85) | 6,900 | 11,800 | 24,000 | 1.15 |
| PEO-PtBA | 15,000 | 17,000 | 23,000 | 1.18 |

Table 3.2: Summary of polyether polyacrylate block copolymers and PtBA homopolymers

### 3.9 Conclusions

All homopolymers and polyether-polyacrylate block copolymers were synthesized successfully. ATRP techniques were successfully utilized to synthesize PtBA using brominated polyethers. The free radical polymerization of *tert*-butyl acrylate was "controlled" but their appears to be some chain combination that made the measured molecular weights considerably higher than the theoretical values (based on assuming no coupling). The polydispersities were low indicating that the amount of chain combination was minimized. Both pentablocks and diblocks yielded consistent high conversions of monomer. Furthermore, these polyether-polyacrylate block copolymers can now be combined in an ionic condensation with drug to form polymer-antibiotic nanoplexes.

# Chapter 4: Release Studies of Gentamicin from Block Ionomer-Antibiotic Nanoplexes as a Function of pH

## 4.1 Abstract

Many pathogenic bacteria can enter phagocytic cells and replicate in them, and these intracellular bacteria are difficult to treat because the recommended antibiotics do not transport into the cells in sufficient concentrations to be efficacious. Examples include food-borne bacteria such as *Salmonella* and *Listeria* as well as more toxic bacteria such as *Brucella* and the *Mycobacteria* that lead to tuberculosis. Current treatments utilize aminoglycoside antibiotics that are polar and positively charged and such drugs do not enter the cells in sufficient concentrations to eradicate the intracellular infections. We have developed core-shell polymeric drug delivery vehicles containing gentamicin to potentially overcome this challenge. Pentablock and diblock copolymers comprised of amphiphilic nonionic polyether blocks and anionic poly(sodium acrylate) blocks have been complexed with the cationic aminoglycoside gentamicin. The electrostatic interaction between the anionic polyacrylates and the cationic aminoglycosides form the cores of the nanoplexes, while the amphiphilic nature of the polyethers stabilize their dispersion in physiological media. The amphiphilic nature of the polyethers in the outer shell aid in interaction of the nanoplexes with extra- and intra-cellular components and help to protect the electrostatic core from any physiological media. This chapter investigates the electrostatic cooperativity between the anionic polyacrylates and cationic aminoglycosides and evaluates the release rates of gentamicin as a function of pH.

## 4.2 Introduction

Many pathogenic bacteria can enter immune cells and replicate in them. These intracellular bacteria are difficult to treat because they can evade the host's natural defenses. Gram-negative and Gram-positive food-borne bacteria, such as *Salmonella* and *Listeria* respectively,are examples. Some fractions of them ultimately reside and replicate within phagocytic cells.[83] Current antibiotics used to treat Gram-negative bacterial infections include gentamicin sulfate, among the aminoglycoside class of antibiotics.[1] Gentamicin is a compound comprised of three sugar groups and five amino groups. At physiological pH the amino groups are protonated and the drug has an overall positive charge. Consequently, this positive charge poses problems for the uptake of the antibiotic into the target cells because polar antimicrobials do not substantially transport

through hydrophobic cell membranes.[2] As a result, free gentamicin introduced as the gentamicin sulfate salt has limited antimicrobial effect on intracellular bacteria. Complete eradication of the bacteria is not achieved and the bacteria continue to harm the individual.

Drug encapsulation by polymers has been reported to be an effective method to increase drug accumulation within the target location.[84-87] To be an effective design, the polymer carrier must avoid detection of the host's immune system and also deliver the antimicrobials to the target cells. Additionally, the therapeutic agent should be engineered to incorporate high concentrations of gentamicin to meet effective dose levels and release gentamicin in a controlled fashion. Controlled delivery and release are necessary to increase the efficacy of gentamicin.

At physiological pH, polyether-polyacrylate block copolymers have an overall negative charge due to carboxylate groups. In an ionic condensation, the polymers and gentamicin can be combined to form a core-shell polymer-antibiotic nanoplex, figure 4.1.

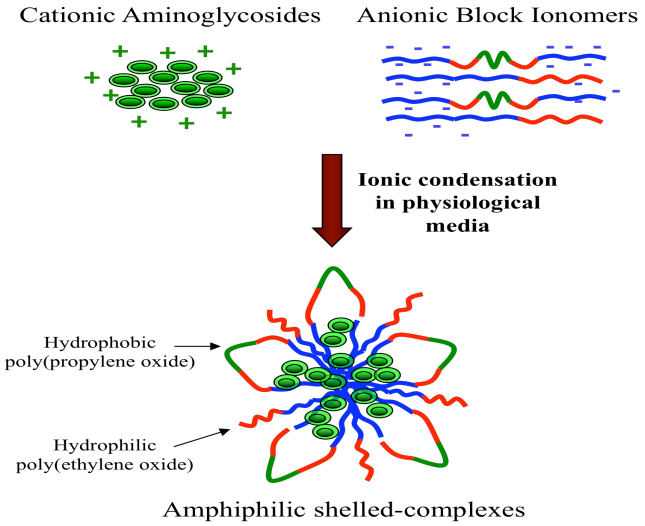


Figure 4.1: Ionic condensation of cationic gentamicin with anionic polyether-polyacrylate block copolymers

When the anionic copolymers are combined with the cationic gentamicin, the drug and polyacrylate segments of the copolymer collapse into the core of core-shell nanoplexes and we hypothesize that the nonionic polyether blocks surround the core and interact with the environment (the medium). These shells are comprised of a combination of PEO and PPO blocks, so the polyether combination produces a micelle that has an amphiphilic nonionic shell. The PPO segments are hydrophobic in nature and can interact with each other and also with a hydrophobic cellular membrane, whereas the hydrophilic PEO provides the needed solubility and steric stabilization to control nanoplex dispersion.

The core-shell nanoplexes were fabricated by two techniques: a batch method and a continuous engineering process. The batch method involved adding a solution of the cationic drug drop-wise to a stirring solution containing the total amount of polymer. Particle nucleation occurs immediately. However, as more gentamicin is added to the polymer solution, the mixture contains a gradually increasing ratio of drug to polymer. The initial drops of gentamicin may condense more efficiently, whereas the final drops might produce nanoplexes that are more loosely bound. As a result, the nanoplexes may be more heterogeneous when they are prepared by the batch method.

It was reasoned that the continuous process may help to avoid compositional heterogeneity among the nanoplexes, principally due to a constant ratio of polymer to drug throughout the process. We employed a small intensive mixer that was originally developed by Prud'homme et al.[88] The continuous process utilizes a four-inlet vortex mixer (figure 4.2) wherein the polymer solution and the gentamicin sulfate solution are continuously fed into a turbulent mixing zone where the particles form rapidly, then the

solution continuously exits the vessel.[88] The approach is to bring the polymer and drug together at a constant ratio under conditions where the mixing time is faster than particle nucleation and growth. The process ensures that polymer and drug meet in a constant charge ratio to enable better homogeneity throughout the nanoplexes.[68]

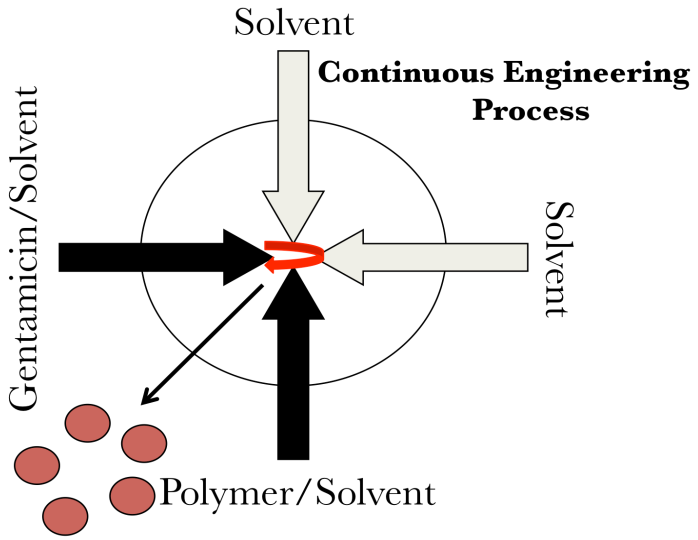


Figure 4.2: A schematic representation of a multi-inlet vortex mixer. This mixer relies on the turbulent mixing of four streams to fabricate polymer-antibiotic nanoplexes

This chapter describes the formation of block copolymer-drug nanoplexes that are bound through cooperative electrostatic attractive forces between the polyacrylate segments of the copolymers and the cationic drug. It is hypothesized that the relatively hydrophobic PPO block of the nonionic polyether also aids in nanoplex stability in aqueous media. Sizes, loading efficiencies, stabilities under simulated physiological conditions, and release times were compared for nanoplexes fabricated by the batch vs. continuous method. Dynamic light scattering was utilized to study the sizes of the nanoplexes at pH 5. Release of the drug from the nanoplexes as a function of pH and as a function of their fabrication method was compared.

## 4.3 Experimental

*4.3.1 Materials*

Monobasic potassium phosphate, dibasic sodium phosphate, potassium chloride, sodium chloride, boric acid, sodium hydroxide, *o*-phthalaldehyde and mercaptoethanol (98 %) were purchased from Sigma-Aldrich and used as received. Gentamicin sulfate (Bioworld, neat salt) was used as received. Isopropanol (Fisher, HPLC grade) was used as received.

*4.3.2 Characterization*

The solute sizes of the complexes were characterized by DLS with a Zetasizer 1000 HS with laser diffractometry (Malvern Instruments, Malvern, UK) at a scattering angle of 177 or 178°. All samples were dispersed in 1.0 mL of phosphate buffered saline, pH 7.4, and filtered through a 1.0 μm PTFE micro-tip filter, and sonicated for 30 minutes prior to analysis. Measurements were done in triplicate for each batch of particles, and the results were taken as the average of three measurements. After derivatization of gentamicin with phthalaldehyde/mercaptoethanol, the gentamicin concentrations were studied by UV-Vis spectroscopy with a UV-1601 Ultraviolet-Visible Spectrophotometer (Shimadzu Instruments). Measurements were done in triplicate and the results are reported as the average of three measurements.

*4.3.3 Preparation of Buffer Solutions*

*4.3.3.1 Preparation of Phosphate Buffered Saline, pH 7.4*

In a 1-L volumetric flask equipped with a magnetic stir bar, sodium chloride (8 g), potassium chloride (0.20 g), dibasic sodium phosphate (1.44 g) and monobasic potassium phosphate (0.24 g) were dissolved in 800 mL of deionized water and stirred. The pH was 7.38. The solution was then diluted to 1 L with deionized water and the measured pH

was 7.39. The final concentration was 11.9 mM phosphate and 139.0 mM sodium chloride.

*4.3.3.2 Preparation of Borate Buffer Solution, pH 9.7*

In a 500-mL Erlenmeyer flask equipped with a magnetic stir bar, boric acid (12.43 g) was dissolved in 400 mL of deionized water. Initially the pH was 4.30 and this was increased by adding a 10 M sodium hydroxide solution (12.5 mL) until the final pH read 9.7. The solution was diluted to 500 mL with deionized water.

*4.3.4 Fabrication of Polymer-Antibiotic Nanoplexes*

*4.3.4.1 Fabrication of Polymer-Antibiotic Nanoplexes Via a Batch Method*

A PAA-*b*-PEO-*b*-PPO-*b*-PEO-*b*-PAA pentablock copolymer, derived from Pluronic P85, with block molecular weight of approximately 9,000 g $mol^{-1}$ and a PAA-*b*-PEO diblock copolymer with block molecular weights of 10,600 g $mol^{-1}$ were utilized to fabricate polymer-antibiotic nanoplexes. The polyether-polyacrylate block copolymers (60 mg each) were dissolved in PBS (30 mL, pH 7.4) to yield a 2.0 mg/mL solution and the solution was stirred overnight at 4 °C. In a 25-mL round-bottom flask equipped with a magnetic stir bar, gentamicin sulfate (0.082 g, 0.049 g gentamicin), in a 1:1 ammonium to carboxylate charge ratio to polymer, was dissolved in PBS (5 mL, pH 7.4) and was stirred overnight at 4 °C.

The solutions were allowed to warm to room temperature and the gentamicin solution was added to the stirring polymer solution drop-wise. The combined solution turned from clear to turbid as the complexes formed. The solution was allowed to stir for an hour and was then placed in the refrigerator at 4 °C. The final concentrations of polymer and gentamicin were 1.71 mg/mL and 1.43 mg/mL respectively, with a final

overall concentration of 3.14 mg/mL. The complex sizes were measured by dynamic light scattering at 25 °C and 37 °C immediately after their fabrication in PBS (pH 5.0) at a concentration of 1.0 mg/mL and at 37 °C for seven days at pH 5.0 to investigate size variation as a function of time. The intensity average diameters were 184 nm at 25 °C and 188 nm at 37 °C immediately after fabrication.

*4.3.4.2 Fabrication of Polymer-Antibiotic Nanoplexes Via a Continuous Engineering Method*

The polymer-antibiotic nanoplexes were also fabricated via a continuous engineering process, which utilizes a multi-inlet vortex mixer. In a 50-mL round-bottom flask equipped with a magnetic stir bar, the polyether-polyacrylate pentablock and diblock copolymers (50 mg each) were dissolved in PBS (30 mL, pH 7.4) to yield a 3.3 mg/mL solution and the solution was stirred overnight at 4 °C. In a separate 50-mL round-bottom flask equipped with a magnetic stir bar, gentamicin sulfate (0.136 g, 0.081 g gentamicin) was dissolved in PBS (25 mL, pH 7.4) and was stirred overnight at 4 °C. The amount of gentamicin and polymers represented a 1:1 cation to anion ratio. The solutions were allowed to warm to room temperature before use.

The continuous engineering process uses four inlets that coalesce at a central mixing point. To ensure optimum nucleation, the flow rates of all four inlets must be controlled as well as the Reynolds number. For this experiment, two inlets pumped PBS (15 mL, pH 7.4) at a flow rate of 10.80 mL/min while the other two inlets pumped the block copolymers (25 mL, 4 mg/mL) and gentamicin sulfate (25 mL, 3.28 mg/mL) solutions at a flow rate of 3.30 mL/min all at 25 °C. The Reynolds number was approximately 3,757. The final concentrations of polymer and gentamicin were 1.41 and

1.162 mg/mL respectively with a final overall concentration of 2.58 mg/mL. The final solution was slightly turbid and the solution was stored in the refrigerator at 4 °C. The complex sizes were measured by dynamic light scattering at 25 °C and 37 °C immediately after fabrication in PBS (pH 5.0) at a concentration of 1.0 mg/mL and at 37 °C for seven days at pH 5.0. The intensity average diameters immediately after fabrication were 127 nm at 25 °C and 178 nm at 37 °C.

*4.3.4.3 Isolation of Polymer-Antibiotic Nanoplexes*

The nanoplexes were purified by a Marathon 21K centrifuge from Fischer Scientific, at 13,300 rpm. Millipore centrifuge filter tubes that contained a 3,000 MWCO membrane were used in the purification process. The membrane serves as a barrier that separates the drug-loaded nanoplexes from smaller structures in the dispersion. PBS and any free gentamicin salts should pass through the membrane due to their low molecular weights. This process leaves behind a pellet comprised of loaded polymer-antibiotic nanoplexes. At 4 mL per run, 20 mL of each nanoplex solution made by each fabrication process was spun at 4,000 rpm (300 $m/s^2$) until all of the eluate passed through the membrane. The eluate was collected and assayed for gentamicin. The eluate from the nanoplexes made by the continuous engineering process contained 25.4 % of the charged gentamicin and the eluate from the nanoplexes made by the batch method contained 31.5 % of the charged gentamicin.

The pellets were re-dispersed in deionized water and lyophilized at -40 °C under reduced pressure. Fifty mg of nanoplexes were recovered from the batch fabrication and 45 mg were recovered from the continuous engineering process. The complex sizes were measured by dynamic light scattering at 37 °C and pH 5.0 in PBS at a concentration of

1.0 mg/mL. The intensity average diameters of the nanoplexes made via the continuous engineering process were 81 nm and those made via the batch method were 122 nm after centrifugation and lyophilization. Additionally, the loading efficiency of the nanoplexes fabricated by the continuous process was 26.6 % by weight gentamicin and 23.3 % by weight gentamicin for the batch process.

*4.3.5 Measurement of Gentamicin Release from the Nanoplexes*

*4.3.5.1 Constructing a Calibration for Assaying Gentamicin*

A gentamicin calibration curve was constructed to assay the amount of gentamicin in the nanoplexes and to assay the amounts released over time. An *o*-phthalaldehyde (OPA) assay was used to measure the amount of gentamicin in each sample.[89] Gentamicin is comprised of three sugar units and five amino groups and is not UV-Vis active. The OPA assay derivatizes the three primary amino groups on the drug and provides a sensitive method to analyze the concentrations by UV spectroscopy.

An OPA solution was prepared by adding phthalaldehyde (3.0 mL, 2.53 x $10^{-2}$ mol) to a scintillation vial followed by mercaptoethanol (15 μL, 2.13 x $10^{-5}$ mol) and the solution was stirred at room temperature for one hour. In a 20-mL scintillation vial equipped with a magnetic stir bar, gentamicin sulfate (16.6 mg, 10 mg gentamicin, 1.57 x $10^{-5}$ eq of primary amino groups) was dissolved in borate buffer (10 mL, pH 9.7) and stirred to make a 1 mg/mL stock solution. From this, a series of dilutions were performed to yield the necessary gentamicin concentrations used for the calibration curve 31.3, 20.8, 15.7, 10.4, 7.8, 5.6, and 3.7 μg/mL. From each solution, 0.5 mL aliquots were taken and placed in separate scintillation vials. To these solutions 0.5 mL of the OPA solution was added followed by 0.2 mL of isopropanol. The isopropanol was added to keep the

derivatized gentamicin in solution. Finally, the solutions were diluted to 3 mL with borate buffer, pH 9.7, and allowed to react for one hour prior to UV-Vis spectroscopy measurements. The absorption was measured at 340 nm.

*4.3.5.2 Release Protocol for Polymer-Antibiotic Nanoplexes as a Function of pH*

*4.3.5.2.1 Release Studies at pH 7.4*

Release studies of the nanoplexes fabricated by each method were conducted at pH 7.4. The studies were carried out over at least 24 hours at 37 °C. The nanoplexes (5.0 mg) were dissolved in PBS (3 mL, pH 7.4) and were placed in a 3,500 MWCO dialysis bag. The dialysis bag was then sealed and placed in a 50 mL beaker containing PBS (50 mL, pH 7.4). The beaker was covered with parafilm and placed in a temperature-controlled shaker and agitated at 80 rpm.

Each hour for the first six hours and once every six hours thereafter, a 0.5 mL aliquot was taken from the receptive media and placed in a scintillation vial. PBS (0.5 mL, pH 7.4) was added back into the beaker to retain a constant volume each time. The aliquot was assayed for gentamicin content via the OPA assay. Briefly, 0.5 mL of the OPA solution was added to each scintillation vial followed by 0.2 mL isopropanol and diluted to 3 mL with borate buffer pH 9.7. The samples were allowed to react for one hour prior to measuring the absorption at 340 nm by UV-Vis spectroscopy.

*4.3.5.2.2 Release Studies at pH 4.5*

The same protocol was followed for the release studies at pH 4.5 over 24 hours at 37 °C. The nanoplexes (5.0 mg) were dissolved in PBS (3 mL, pH 4.5) and were placed in a 3,500 MWCO dialysis bag. The dialysis bag was sealed and placed in a 50-mL beaker containing PBS (50 mL, pH 4.5). The beaker was covered with parafilm and

placed in a temperature-controlled shaker and agitated at 80 rpm. Each hour for the first six hours and once every six hours thereafter, a 0.5 mL aliquot was taken from the receptive media and placed in a scintillation vial. PBS (0.5 mL, pH 4.5) was added back into the beaker to retain a constant volume each time. This aliquot was then assayed for gentamicin content via the OPA assay discussed above.

## 4.4 Results and Discussion

### *4.4.1 Comparison of the Batch and Continuous Fabrication Methods*

A batch and a continuous method were utilized to prepare the polymer-antibiotic nanoplexes and the resulting materials were compared. The batch method relies on addition of an antibiotic/PBS solution to a stirring polymer/PBS solution. By contrast, the continuous engineering process uses a multi-inlet vortex mixer that combines polymer, drug, and solvent continuously from four streams. Table 4.1 displays a comparison of properties of nanoplexes produced immediately after each fabrication process and before centrifugation. The same polyether-polyacrylate block copolymers were used in a 1:1 wt:wt ratio in both methods. Additionally, the ratio of ammonium cations to acrylate anions charged in both processes was kept constant at 1:1.

| Polymers | Fabrication Method | Charge Ratio | Polymer Wt. Ratio | Intensity Ave. Diameter 37 °C (nm) |
|---|---|---|---|---|
| $PAA_{27}$-Polyether-$PAA_{27}$/ PEO-$PAA_{117}$ | Continuous | 1:1 Anion/Cation | 1:1 | 178 |
| $PAA_{27}$-Polyether-$PAA_{27}$/ PEO-$PAA_{117}$ | Batch | 1:1 Anion/Cation | 1:1 | 188 |

Table 4.1: Summary of data compiled from the fabrication of polymer-antibiotic nanoplexes via a continuous and batch process

Dynamic light scattering was utilized to measure the hydrodynamic sizes of the nanoplexes immediately after fabrication at 37 °C. The sizes produced by both methods

were approximately the same. The continuous engineering process had an average intensity diameter of 178 nm, whereas the batch process produced sizes of 188 nm.

Additionally, the intensity hydrodynamic diameters of the nanoplexes were studied as a function of time. The nanoplexes were aged in PBS at pH 5 for seven days in a temperature controlled environment at 37 °C and were shaken at 80 rpm. Table 4.2 displays the results of this experiment. Under these conditions, the nanoplex sizes are stable. At this pH, a portion of the polyacrylic acid units are in the acid form and hydrogen bonds between the carboxylic acids and the polyether units may be important to enhance this stability.

| Fabrication Method | Day 1 | Day 2 | Day 3 | Day 4 | Day 5 | Day 6 | Day 7 |
|---|---|---|---|---|---|---|---|
| Continuous | 178 | 168 | 220 | 218 | 208 | 195 | 203 |
| Batch | 188 | 172 | 180 | 181 | 240 | 179 | 220 |

Table 4.2: Summary of data of the size intensity averages of unpurified nanoplexes from each fabrication technique. The nanoplexes were aged at 37 °C for seven days.

The sizes of the nanoplexes were also studied at pH 7.4. Originally, the nanoplexes had a pH of 5.0 in the PBS. The pH was brought up from 5.0 to 7.4 by addition of sodium hydroxide solution and the sizes were measured at 37 °C. At pH 5.0, the intensity average diameters of the nanoplexes were approximately 180 nm, whereas at pH 7.4, the intensity average diameters increased to 2,000 nm. This can at least be partially attributed to the hydrophobicity of the PPO segments. The nanoplexes are indeed more stable at pH 5.0 but begin to aggregate tremendously at pH 7.4.

Although the particles have the same diameter, they are stable at pH 5.0 and less stable at pH 7.4, there are still differences between the two. The batch method relies on addition of the gentamicin to a stirring polymer solution. All of the polymers are in the polymer solution from the beginning of the addition of drug, so the ratio of polymer to

drug decreases throughout the fabrication process. This change in ratio may disrupt the homogeneity of the resulting nanoplexes. More polymer is available to encapsulate the drug relative to the overall 1:1 charge ratio. However, as more gentamicin is added the homogeneity changes as less polymer is available to encapsulate gentamicin. This might result in poor encapsulation efficiency, as gentamicin is not incorporated into the core of the nanoplex. This change in homogeneity might affect the release of gentamicin, as there is a more heterogeneous nanoplex.

Conversely, the continuous engineering process uses turbulent mixing of polymer and drug to ensure a more homogeneous environment for complex nucleation. The ratio of polymer to drug entering the mixer remains constant throughout the process. Keeping the ratio more consistent helps ensure a more homogeneous particle. These particles have more of a homogeneous topology and thus might have a better sustained release. If the particle is more homogeneous, then gentamicin may release more effectively, and this is borne out in the results of the release experiments described herein.

To examine the efficiency of gentamicin release from the nanoplexes, the concentration of gentamicin was measured through an OPA assay. Gentamicin is not UV-Vis active and must be functionalized to absorb light in the UV-Vis range. The OPA assay uses phthalaldehyde and mercaptoethanol to react with the primary amines of gentamicin, (figure 4.3). The OPA assay offers a highly sensitive method for detecting primary amines, such as those on proteins, peptides and aminoglycosides.[90] The gentamicin-phthalaldehyde-mercaptoethanol derivative is soluble and stable in aqueous solutions at basic pH's and it absorbs strongly in the UV range.[91-94] In the presence of mercaptoethanol, OPA reacts with primary amines in their free amino form. At pH 9.7,

the ammonium groups of gentamicin are deprotonated to yield two secondary amines and three primary amines. Others have previously demonstrated that the OPA assay reacts with all three primary amines.[90] The derivatization of the primary amines with OPA was monitored by the absorption band at 340 nm.

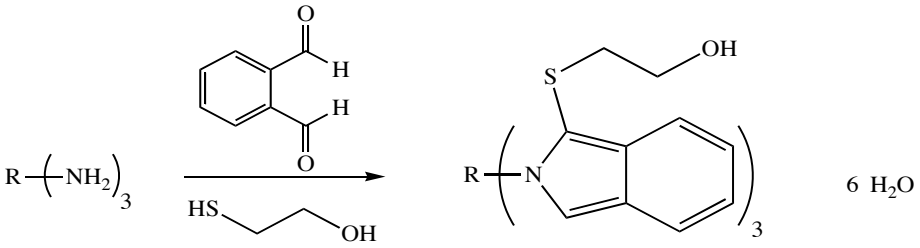


Figure 4.3: Synthetic scheme of the reaction of the primary amines of gentamicin with phthalaldehyde and mercaptoethanol.

A calibration curve was constructed to determine the gentamicin content loaded in the nanoplexes and free drug in the eluate after the centrifugation (isolation) procedure, (figure 4.4). The calibration points ranged from 0.62 μg/mL of gentamicin to 5.22 μg/mL and this resulted in a linear regression correlation of 99.55%. The linear regression was then used to quantify the amount of gentamicin in the nanoplexes. Table 4.3 summarizes the results of the gentamicin assays to establish the amount of drug in the nanoplexes after isolation. Both fabrication methods produced nanoplexes that contained approximately the same concentration of gentamicin.

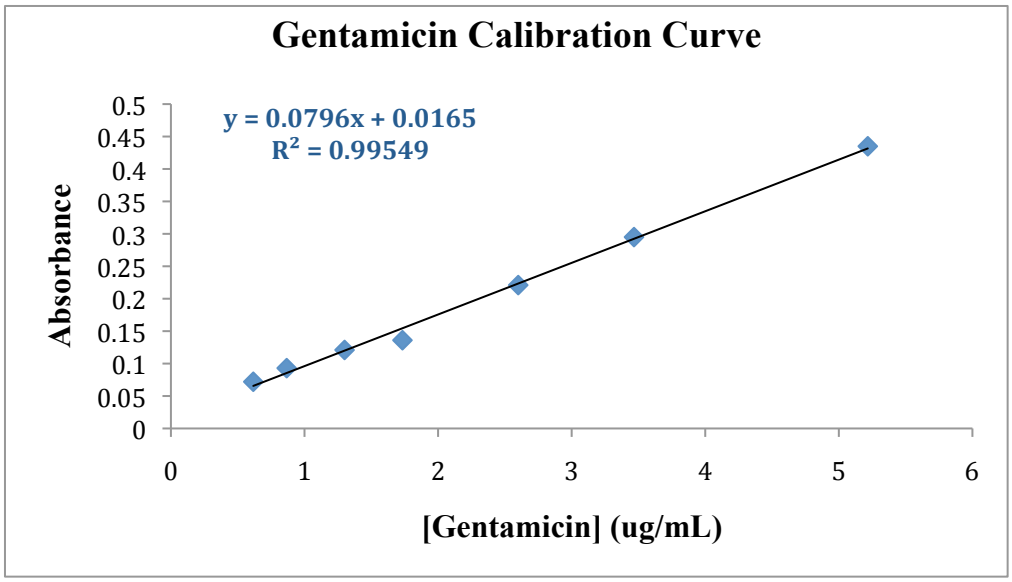


Figure 4.4: Gentamicin Calibration Curve

| Polymers | Fabrication Method | % Gentamicin Removed During Centrifugation | % Gentamicin Remaining After Centrifugation | Wt. % Gentamicin Charged in Complex | Wt % Gentamicin in the Complex |
|---|---|---|---|---|---|
| $PAA_{27}$-Polyether-$PAA_{27}$/ PEO-$PAA_{117}$ | Continuous | 25.4 | 74.6 | 50.0 | 26.6 |
| $PAA_{27}$-Polyether-$PAA_{27}$/ PEO-$PAA_{117}$ | Batch | 31.5 | 68.5 | 50.0 | 23.3 |

Table 4.3: Comparison of loading capacities of gentamicin through both fabrication methods

*4.4.2 Comparison of Release Efficiencies of Gentamicin from the Nanoplexes at pH 7.4*

The amounts of gentamicin released were measured as a function of pH over time utilizing the OPA assay of the derivatized drug. The nanoplexes were placed in a cellulose acetate dialysis bag with a MWCO of 3,000 g $mol^{-1}$ so that only the small molecule drugs, and not the polymers or the nanoplexes containing polymer, could pass through the membrane. The released gentamicin was measured over at least 24 hours. Figure 4.5 shows the release from the nanoplexes fabricated by the batch method at pH 7.4. Initially, there is a burst release of approximately 20 % of the total amount of drug

contained, and this was followed by release to approximately 40 % by five hours and little to no further release thereafter.

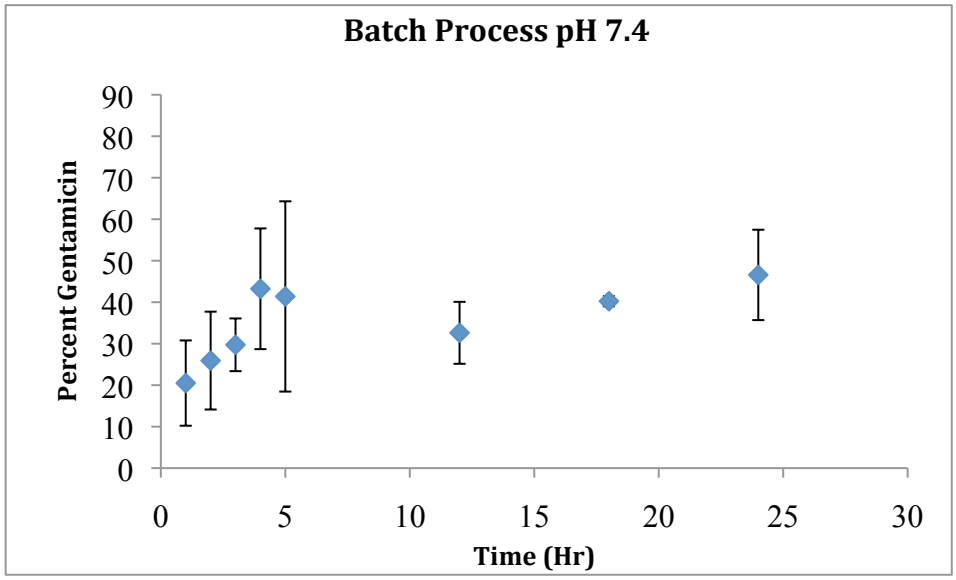


Figure 4.5: Release of gentamicin from nanoplexes made through a batch method at pH 7.4. The error bars are representative of the standard deviation of three separate experiments.

These results suggest that the nanoplexes may contain some loosely-bound drug that releases quickly. Toward the end of the fabrication process the drug to polymer ratio becomes lower than at the beginning. As a result, some drug may not be condensed into the core of the nanoplex efficiently. The minimal release between five and 24 hours suggests that some of the drug may also be bound too tightly in the core. The cooperativity of electrostatic attractions in the core might be too strong and therefore limit the release of the drug into solution.

In comparison to the batch-fabricated nanoplexes, those made via the continuous engineering process exhibited significantly improved overall release results (figure 4.6). The same trend persisted for the first several hours. Initially, a burst release occurs releasing approximately 30 % gentamicin and this followed by release up to about 40% by the five-hour measurement. However, over 24 hours, the overall release of gentamicin

is significantly higher for the complexes prepared with the constant ratio of polymer to drug. Over the 48 hours, the total release is approximately 75 %. These results suggest that the continuous engineering process may have produced nanoplexes with better homogeneity over their distribution. The sustained release may be critically important for achieving the desired intracellular drug concentrations over time *in vitro* and *in vivo*.

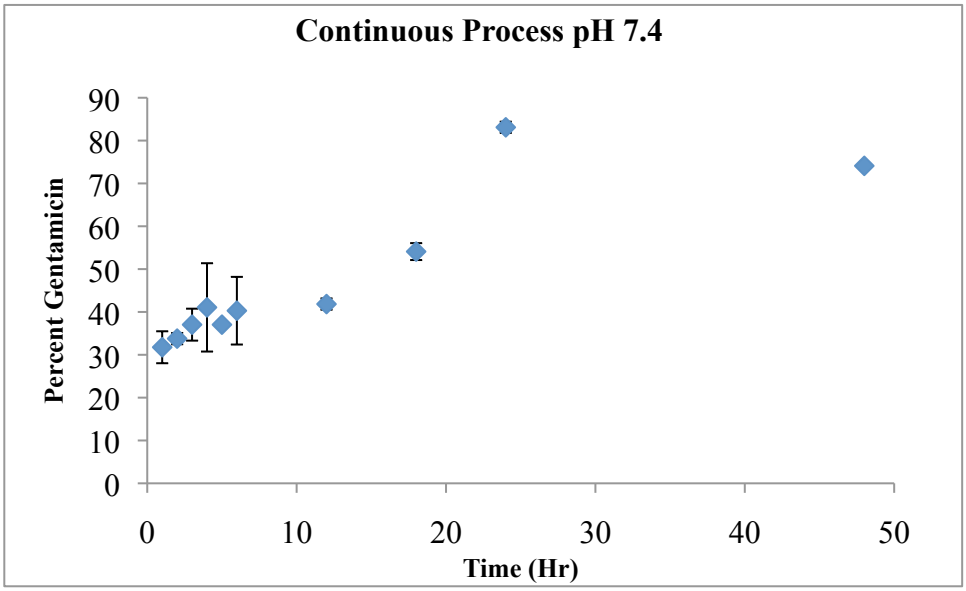


Figure 4.6: Release efficiencies at pH 7.4 of gentamicin from nanoplexes made through a continuous engineering process. The error bars represent the standard deviation based on two separate experiments. The point at 48 hours was only measured once.

*4.4.3 Comparison of Release Efficiencies of Gentamicin from the Nanoplexes at pH 4.5*

Release comparisons for gentamicin from the nanoplexes were also conducted at pH 4.5. This pH was used to simulate the intracellular pH of the target phagocytic cells. Figure 4.7 shows the results of the release experiment of the nanoplexes synthesized through the batch method. The results show an initial burst release followed by little to no additional change over 24 hours. The overall amount of release for the complexes prepared by the batch method at pH's of 7.4 and 4.5 were comparable.

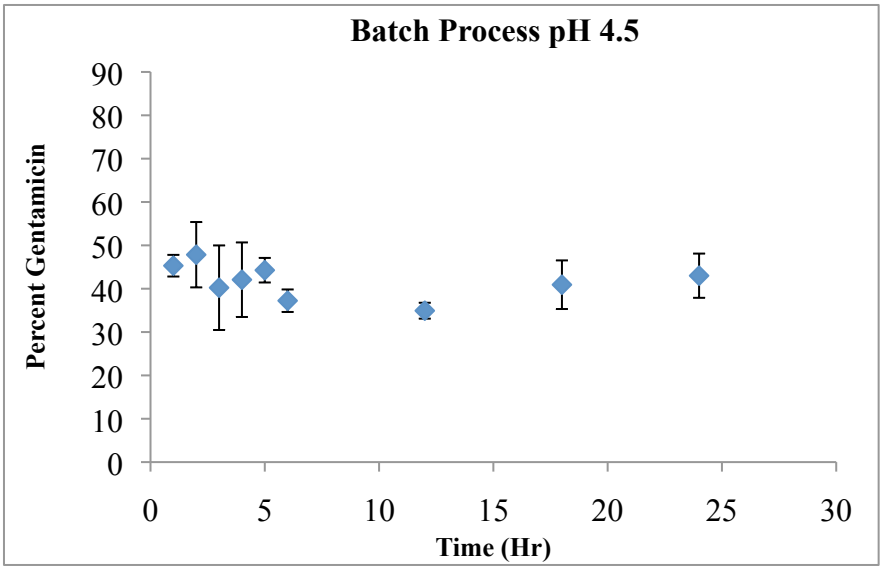


Figure 4.7: Release efficacies of gentamicin from nanoplexes made through a batch method at pH 4.5. The error bars are representative of the standard deviation of three separate experiments.

Additionally, the release results of the nanoplexes synthesized via the continuous engineering process showed similar results at the lower pH. An initial burst release was observed within the first several hours followed by little to no further release over 24 hours (figure 4.8).

It is well documented in the literature that the oxygens of PEO hydrogen bond readily to the carboxylic acid groups of polyacrylic acid.[81] At pH 4.5, the carboxylates begin to protonate ($pK_a = 4.76$), shown in figure 4.9. As more carboxylic acids form, the hydrogen bonding increases. This relationship might explain the data observed in both experiments at pH 4.5. The initial burst release can at least be partially attributed to dissociation of the drug from the polymer as the polymer begins to protonate. It is reasoned that the drug may become trapped within the core of the complex as the polyacrylic acid begins to hydrogen bond to PEO to form a hydrogen-bonded network. The limited release at pH 4.5 could be due to encapsulation of gentamicin within a

hydrogen-bonded core and being electrostatically bound to the remaining carboxylate groups.

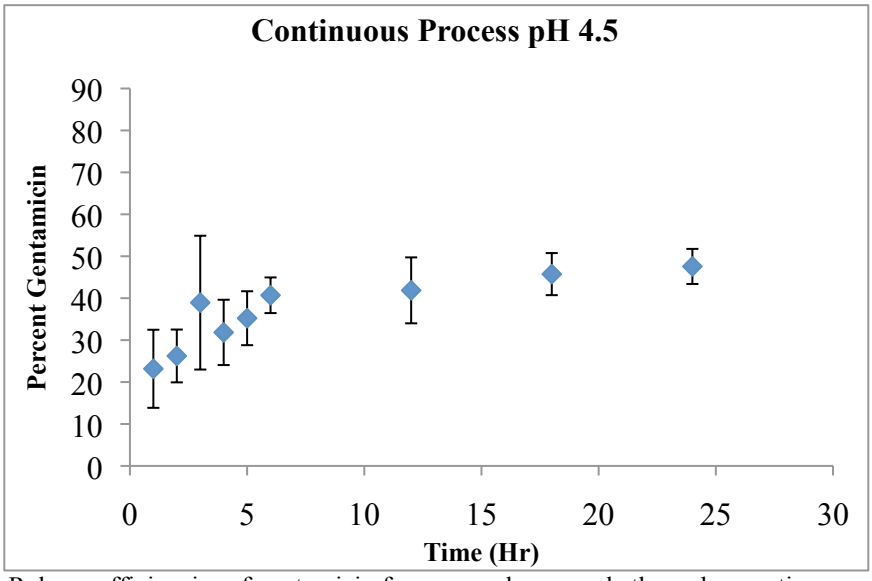


Figure 4.8: Release efficiencies of gentamicin from nanoplexes made through a continuous engineering process at pH 4.5. The error bars are representative of the standard deviation of three separate experiments.

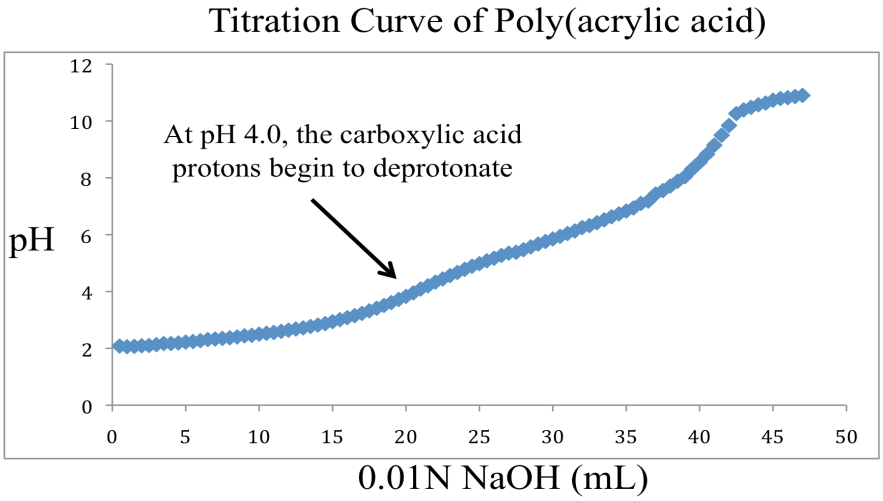


Figure 4.9: Titration curve of poly(acrylic acid)

## 4.5 Conclusions

Both fabrication techniques, continuous and batch, were successfully utilized to synthesize core-shell polymer-antibiotic nanoplexes containing high concentrations of gentamicin. Both processes produced nanoparticles through ionic condensation of polymer with drug. The nanoplexes were purified by centrifugation through a membrane

with a low molecular weight cut-off value so that any free (unencapsulated) drug could be removed. The overall weight percent of gentamicin in the complexes was very high, 26.6 % and 23.3 % in the continuous and batch sets respectively. The sizes of the nanoplexes immediately after fabrication were measured by DLS at pH 5.0 and 7.4. They were found to be more stable at pH 5.0 than at pH 7.4, and this was attributed to hydrogen bonding of the acrylic acid groups with PEO at the lower pH. Release studies of gentamicin all of the release experiments showed an initial burst release. At pH 7.4, release from the nanoplexes fabricated in the continuous process were substantially improved over the batch process, likely a result of improved homogeneity in those systems. At pH 4.5, both sets of materials showed very little further release after the first few hours. This may be attributable to the formation of hydrogen-bonded networks at the lower pH.

## Chapter 5: Conclusions

### 5.1 Summary

This research focused on the synthesis of block copolymers comprised of polyether and polyacrylate blocks and their fabrication into core-shell nanostructures where the core contained high loadings (~25 wt%) of the cationic antibiotic, gentamicin. Gentamicin is one of the recommended drugs for treating important bacterial infections including brucellosis and salmonellosis. However, while gentamicin can effectively treat extracellular *brucella* and *salmonella*, it's polar cationic nature inhibits its transport into cells. These bacteria partially reside and replicate inside phagocytic host cells and free gentamicin does not enter these cells in sufficiently high concentrations to be effective at eradicating the bacteria. Thus, our goal was to design a core-shell nanostructure where the drug could be encapsulated into the core, and the shell would interact with the cells and aid in transporting the drug-carrier vehicles into the cells.

The polyether-polyacrylate block copolymer carriers were synthesized by forming alkyl bromide-functional macroinitiators from hydroxyl-terminated polyethers and polymerizing *t*-butyl acrylate by atom transfer free radical polymerization. In the presence of a Cu(I)Br/ligand complex, *tert*-butyl acrylate was initiated from a tertiary bromide on the macroinitiators and polymerized. Monomer conversions were taken to 70-90 %. Under these conditions, the ATRP polymerization underwent some termination, presumably by chain coupling, so the molecular weights that were obtained were somewhat higher than anticipated. However, the ATRP reaction did afford block copolymers that were shown to be useful for producing the desired nanostructures with the aminoglycoside. Following polymerization of the *t*-butyl acrylate, the *t*-butyl groups

were removed with trifluoroacetic acid in organic media.

At physiological pH, gentamicin has five positive ammonium ions, whereas the polyacrylate blocks of the copolymers have multiple anionic carboxylates. Through ionic condensation, the cationic drug was complexed with these anionic polyacrylate blocks. Core-shell polymeric nanostructures resembling micelles were formed that housed a charged core containing the drug, and the nonionic polyether shells afforded dispersion of the complexes in physiological media.

Two fabrication methods for the nanostructures were compared: a batch method and a continuous engineering method. The batch method was conducted by adding the drug drop-wise to a polymer solution, and the continuous process relied on rapid turbulent mixing of the polymers and drug as they entered the mixing chamber. In the batch method, the ratio of drug to polymer increased during the addition, while the continuous method was conducted such that the drug to polymer ratio remained constant throughout. The rates and efficiencies of drug release from these nanoplexes were investigated as a function of pH and as a function of the fabrication method. The formation of polymer-antibiotic nanoplexes and release of the drug were studied at pH 7.4 (to simulate physiological pH) and pH 4.5 (to simulate endosomal pH). It was hypothesized that the continuous process would produce a more steady release of gentamicin due to better homogeneity of the nanoplexes. The data support the hypothesis at physiological pH (7.4). At pH 7.4, the nanostructures containing the gentamicin showed an initial burst release, but this was followed by a slow sustained release over 24 hours.

**5.2 Conclusions**

In conclusion, the polymer-antibiotic nanoplexes were successfully formed through ionic condensation of the anionic polymer blocks with the cationic drug. A blend of a diblock having a PEO hydrophilic shell was blended with a pentablock copolymer having an amphiphilic shell. The amphiphilicity of the pentablock copolymer was adjusted to be rather high in the hydrophobic PPO component relative to the hydrophilic PEO components. The strategy was to utilize the relative hydrophobicity of the pentablock copolymer to help hold the nanostructures together to obtain longer sustained release. The hydrophilic diblock copolymer was added to ensure that the nanostructures would remain well dispersed in aqueous physiological media.

Both fabrication techniques, continuous and batch, were successfully utilized to synthesize core-shell polymer-antibiotic nanoplexes containing high concentrations of gentamicin. The overall weight percent of gentamicin in the complexes was very high, 26.6 % and 23.3 % in the continuous and batch sets respectively. The stabilities of the nanoplexes were measured by DLS at pH 5.0 and 7.4. Surprisingly, the nanoplexes were found to be more stable at pH 5.0, and this was attributed to hydrogen bonding between the acrylic acid groups and PEO. Release of the drug at this pH was characterized by an initial burst release, but very little release thereafter. At pH 7.4, dynamic light scattering confirmed that the particles begin to break up more efficiently. The nanoplexes fabricated by the continuous process were found to be superior to those produced in the batch method. An initial burst release was followed by a steady sustained release over 24 hours. By contrast, at pH 7.4, the nanoparticles made in the batch method showed an initial burst but release little drug thereafter.

## REFERENCES


(1) Ranjan, A.; Pothayee, N.; Saleem, M.; Jain, N., Sriranganathan, N.; Riffle, J.S.; Kasimanickam, R. Drug Delivery Using Novel Nanoplexes Against a *Salmonella* Mouse Infection Model. *Journal Nanoparticle Research* **2009**, 12, 905-914.

(2) Lecaroz, C.; Gamazo, C.; Blanco-Prieto, MJ. Nanocarriers with Gentamicin to Treat Intracellular Pathogens. *Jounral of Nanoscience Nanotechnology*. **2006**, 6, 3296-3302.

(3) Kabanov, A.V.; Chekhonin, V.P.; Alakhov, V.Y.; Batrakova, E.V.; Lebedev, A.S.; Melik-Nubarov, N.S.; Arzhakov, S.A.; Levashov, A.V.; Morozov, G.V.; Severin, E.S., Kabanov, V.A. The neuroleptic Activity of Haloperidol Increases After its Solubilization in Surfactant Micelles: Micelles as Microcontainers for Drug Targeting. *FEBS Journal*. **1989**, 258, 343-345.

(4) Yokoyama, M.; Fukushima, S.; Uehara, R.; Okamoto, K.; Kataoka, K.; Sakurai, Y.; Okano, T. Characterization of Physical Entrapment and Chemical Conjugation of Adriamycin in Polymeric Micelles and Their Design for In Vivio Delivery to a Solid Tumor. *Journal of Controlled Release*, **1998**, 50, 79-92.

(5) Yokoyama M.; Satoh, A.; Sakurai, Y.; Okano T.; Matsumura, Y.; Kakizoe, T.; Kataoka, K. Incorporation of Water-Insoluble Anticancer Drug into Polymeric Micelles and Control of Their Particle Size. *Journal of Controlled Release*, **1998**, 55, 219-229.

(6) Li, Y.; Kwon, G.S. Methotrexate Esters of Poly(ethylene oxide)-block-poly(2-hydroxyethyl-L-aspartamide). Part 1: Effects of the Level of Methotrexate Conjugation on the Stability of Micelles and on Drug Release. *Pharmaceuticals Research*, **2000**, 17, 607-611.

(7) Tuzar, Z.; Kratochvil, P. Block and Graft Copolymer Micelles in Solution. *Advanced Colloid Interface Science*, **1976**, 6, 201-232.

(8) Yagusi, K.; Nagasaki, Y.; Kato, M.; Kataoka, K. Preparation and Characterization of Polymer Micelles from Poly(ethylene glycol)-poly(D,L-lactide) Block Copolymers as Potential Drug Carrier. *Journal of Controlled Release*, **1999**, 62, 89-100.

(9) Nishiyama, N.; Yokoyama, M.; Aoyagi, T.; Okano, T.; Sakurai, Y.; Kataoka, K. Preparation and Characterization of Self-Assembled Polymer-Metal Complex Micelle from cis-dichlorodiammineplatinum (II) and Poly(ethylene glycol)-poly(a,p-aspartic acid) Block Copolymer in an Aqueous Medium. *Langmuir*, **1999**, 15, 377-383.

(10) Kataoka, K.; Togawa, H.; Harada, A.; Yasugi, K.; Matsumoto, T.; Katayose, S. Spontaneous Formation of Polyion Complex Micelles with Narrow Distribution from Antisense Oligonucleotide and Cationic Block Copolymer in Physiological Saline. *Macromolecules*, **1996**, 29, 8556-8557.

(11) Harada, A.; Kataoka, K. Novel Polyion Complex Micelles Entrapping Enzyme Molecules in the Core: Preparation of Narrowly-Distributed Micelles from Lysozyme and Poly(ethylene glycol)-poly(aspartic acid) Block Copolymer in Aqueous Medium. *Macromolecules*, **1998**, 31, 288-294.

(12) Kataoka, K.; Harada, A.; Nagasaki, Y. Block Copolymer Micelles for Drug Delivery: Design, Characterization and Biological Significance. *Advanced Drug Delivery Review*, **2001**, 47, 113-131.
(13) Younsoo, B.; Kataoka, K. Intelligent Polymeric Micelles from Functional Poly(ethylene glycol)-poly(amino acid) Block Copolymers. *Advanced Drug Delivery Reviews*, **2009**, 61, 768-784.
(14) Kwon, G., (Ed). Polymeric Drug Delivery Systems. Vol. 148, Taylor and Francis Group, Boca Raton, FL, **2005**, pp. 533-534.
(15) Allen, C.; Maysinger, D.; Eisenberg, A. Nano-engineering Block Copolymer Aggregates for Drug Delivery. *Colloids Surface B Biointerfaces*, **1999**, 16, 3-27.
(16) Nishiyama, N.; Bae, Y.; Miyata, K.; Fukushima, S.; Kataoka, K. Smart Polymeric Micelles for Gene and Drug Delivery. *Drug Discovery Today: Technology*, **2005**, 2, 21-26.
(17) Griffith, L.G.; Polymeric Biomaterials. *Acta Materialia*, **2000**, 48, 263-277.
(18) Yamaoka, T.; Tabata, Y.; Ikada, Y. Distribution and Tissue Uptake of Poly(ethylene glycol) with Different Molecular Weights After Intravenous Administration to Mice. *Journal of Pharmaceutical Science*, **1994**, 83, 601-606.
(19) Riess, G.; Hurtrez, G.; Bahadur, P., (Eds). Encyclopedia of Polymer Science and Engineering, Vol. 2, 2nd Ed., John Wiley and Sons, Inc, New York, **1985**, pp. 324-434.
(20) Cammas, S.; Harada, A.; Nagasaki, Y.; Kataoka, K. Poly(ethylene oxide-co-β-benzyl-L-aspartate) Block Copolymers of Poly(ethylene oxide) and Poly(β-benzyl L-aspartate) Segment in Organic Solvents. *Macromolecules*, **1996**, 29, 3227-3231.
(21) Harada, A.; Cammas, S.; Kataoka, K. Stabilized α-helix Structure of poly(L-lysine)-block-poly(ethylene glycol) in Aqueous Medium Through Supramolecular Assembly. *Macromolecules*, **1996**, 29, 6183-6188.
(22) Yokoyama, M.; Okano, T.; Sakurai, Y.; Kataoka, K. Improved Syntheis of Adriamycin-Conjugated Poly(ethylene glycol)-poly(aspartic acid) Block Copolymer and Formation of Unimodal Micellar Structure with Controlled Amount of Physically Entrapped Adriamycin. *Journal of Controlled Release*, **1994**, 32, 269-277.
(23) Younsoo, B.; Kataoka, K. Intelligent Polymeric Micelles from Functional Poly(ethylene glycol)-poly(amino acid) Block Copolymers. *Advanced Drug Delivery Reviews*, **2009**, 61, 768-784.
(24) Yokoyama, M.; Sugiyama, T.; Okano, T.; Sakurai, Y.; Naito, M.; Kataoka, K. Analysis of Micelle Formation of an Adriamycin-conjugated Poly(ethylene glycol)-poly(aspartic acid) Block Copolymer by Gel Permeation Chromatography. *Pharmaceutical Research*, **1993**, 10, 895-899.
(25) Yokoyama, M.; Fukushima, S.; Uehara, R.; Okamoto, K.; Kataoka, K.; Sakurai, Y.; Okano, T. Characterization of Physical Entrapment and Chemical Conjugation of Adriamycin in Polymeric Micelles and Their Design for a Solid Tumor. *Journal of Controlled Release*, **1998**, 50, 79-92.
(26) Malmstadt, N.; Yager, P.; Hoffman, A.S.; Stayton, P.S. A Smart Microfluidic Affinity Chromatography Matrix Composed of Poly(N-isopropylacrylamide)-Coated Beads. *Journal of Analytical Chemistry*, **2003**, 75, 2943-2949.

(27) Bae, Y.; Okano, T.; Kin S. Insulin Permeation Through Thermosensitive Hydrogels. *Journal of Controlled Release*, **1989**, 9, 271-279.
(28) Lee, Y.; Fukushima, S.; Bae, Y.; Hiki, S.; Ishii, T.; Kataoka, K. A Protein Nanocarrier from Charge-Conversion Polymer in Response to Endosomal pH. *Journal of American Chemical Society*, **2007**, 129, 5362-5663.
(29) Fukushima, S.; Miyata, K.; Nishiyama, N.; Kanayama, N.; Yamasaki, Y.; Kataoka, K. *Journal of American Chemical Society*, **2005**, 127, 2810.
(30) Hruby, M.; Konak, C.; Ulbrich, K. Polymeric Micellar pH-Sensitive Drug Delivery System for Doxorubicin. *Journal of Controlled Release*, **2005**, 103, 137-148.
(31) Chytry, V.; Ulbrich, K. Conjugate of Doxorubicin with a Thermosensitive Polymer Drug Carrier. *Journal Bioactive and Compatible Polymers*, **2001**, 16, 427-440.
(32) Zhao, X.; Pan, F.; Zhang, Z.; Grant, C.; Ma, Y.; Armes, S.; Tang, Y.; Lewis, A.; Waigh, T.; Lu, J. Nanostructure of Polyplexes Formed Between Cationic Diblock Copolymer and Antisense Oligodeoxynucleotide and its Influence on Cell Transfection Efficiency. *Biomacromolecules*, **2007**, 8, 3493-3502.
(33) Pack, D.; Hoffman, A.; Pun, S.; Stayton, P. Design and Development of Polymers for Gene Delivery. *Nature Reviews Drug Delivery*, **2005**, 4, 581-593.
(34) Mehier-Humbert, S.; Guy, R. Physical Methods for Gene Trnasfer: Improving the Kinetics of Gene Delivery into Cells. *Advanced Drug Delivery Reviews*, **2005**, 57, 733-753.
(35) Goverdhana, S.; Puntel, M.; Xiong, W.; Zirger, J.; Barcia, C.; Curtin, J.; Soffer, E.; Mondkar, S.; King, G.; Hu, J.; Sciascia, M. Regulatable Gene Expression Systems for Gene Therapy Applications: Progress and Future Challenges. *Molecular Therapy*, **2005**, 12, 189-211.
(36) Li, S.; Huang, L.; Nonviral Gene Therapy: Promises and Challenges. *Gene Therapy*, **2000**, 7, 31-34.
(37) Dias, N.; Stein, C. Antisense Oligonucleotides: Basic Concepts and Mechanisms. *Molecular Cancer Therapy*, **2002**, 1, 347-355.
(38) Sarkar, T.; Conwell, C.; Harvey, L.; Santai, C.; Hud, N. Condensation of Oligonucleotides Assembled into Nicked and Gapped Duplexes: Potential Structures for Oligonucleotide Delivery. *Nucleic Acids Research*, **2005**, 33, 143-151.
(39) Jessel, N.; Oulad-Abdelghani, M.; Meyer, F.; Lavelle, P.; Haikel, Y.; Schaaf, P.; Voegel, J. Multiple and Time-scheduled In Situ DNA Delivery Mediated by β-cyclodextrin Embedded in a Polyelectrolyte Multilayer. *Proceedings of the National Academy of Science*, **2006**, 103, 8618-8621.
(40) Lucas, B.; Remaut, K.; Sanders, N.; Braeckmans, K.; Smedt, S.; C. D.; Demeester, J. Studying the Intracellular Dissociation of Polymer-Oligonucleotide Complexes by Dual Color Fluorescence Fluctuation Spectroscopy and Confocal Imaging. *Biochemistry*, **2005**, 44, 9905-9912.
(41) Wilson, A.; Zhou, W.; Champion, H.; Alber, S.; Tang, Z.; Kennel, S.; Watkins, S.; Huang, L.; Pitt, B.; Li, S. Targeted Delivery of Oligodeoxynucleotides to Mouse Lung Endothelial Cells In Vitro and In Vivo. *Molecular Therapy*, **2005**, 12, 510-518.

(42) Brus, C.; Peterson, H.; Aigner, A.; Czubayka, F.; Kissel, T. Physicochemical and Biological Characerization of Polyethylenenimine-*graft*-poly(ethylene glycol) Block Copolymers as a Delivery System for Oligonucleotides and Ribozymes. *Bioconjugate Chemistry*, **2004**, 15, 677-684.
(43) Chim, Y.; Lam, J.; Ma, Y.; Armes, S.; Lewis, A.; Roberts, C.; Stolnik, S.; Tendler, S.; Davies, M. Structural Study of DNA Condensation Induced by Novel Phosphorylcholine-based Copolymers for Gene Delivery and Relevance to DNA Protection. *Langmuir*, **2005**, 21, 3591-3598.
(44) Langer, R.; Drug Delivery and Targeting. *Nature*, **1998**, 392, 5-10.
(45) Stolnik, S.; Illum, L.; Davis, S. Long Circulating Microparticulate Drug Carriers. *Advanced Drug Delivery Review*, **1995**, 16, 195-214.
(46) Schmolka, I. A review of Block Copolymer Surfactants. *Journal of American Oil Chemical Society*, **1977**, 54, 110-116.
(47) Geyer, R. Perfluorochemicals as Oxygen Transport Vehicles. *Biomateirals, Artificial Cells, and Artificial Organs*, **1988**, 16, 31-49.
(48) Allison, A.; Byars, N. Adjuvant Formulations and Their Mode of Action. *Seminars in Immunology*, **1990**, 2, 369-374.
(49) Schmolka, I. Physical Basis for Poloxamer Interactions. *Annual NY Academy of Science*, **1994**, 720, 92-97.
(50) Hawley, A.; Davis, S.; Illum, L. Targeting of Colloids to Lymph Nodes: Influence of Lymphatic Physiology and Colloidal Characteristics. *Advanced Drug Delivery Review*, **1995**, 17, 129-148.
(51) Newman, M.; Actor, J. Balusubramanian, M.; Jagannath, C. Use of Nonionic Block Copolymers in Vaccines and Therapeutics. *Critical Reviews of Therapy Drug Carrier Systems*, **1998**, 15, 89-142.
(52) Malmsten, M. Block Copolymers in Pharmaceutics. In: Alxandrisidis, P.; Lindman, B. (Eds). Amphiphilic Block Copolymers: Self Assembly and Applications. Amsterdam, New York; Elesvier, **2000**, pp. 319-346.
(53) Moghimi, S.; Hunter, A. Poloxamers and Poloxamines in Nanoparticle Engineering and Experimental Medicine. *Trends in Biotechnology*, **2000**, 18, 412-420.
(54) Anderson, B.; Pandit, N.; Mallapragada, S. Understanding Drug Release From Poly(ethylene oxide)-b-poly(propylene oxide)-b-poly(ethylene oxide) Gels. *Journal of Controlled Release*, **2001**, 70, 157-167.
(55) Emanuele, M.; Balasubramanian, M.; Alludeen, H. Polyoxypropylene/polyoxyethylene Copolymers with Improved Biological Activity. Norcross, GA, CytoRx Corp, **1996**.
(56) Emanuele, M.; Hunter, R.; Culbert, P. Polyoxypropylene/polyoxyethylene Copolymers with Improved Biological Activity. Norcross, GA, CytoRx Corp, **1996**.
(57) Kabanov, A.; Batrakova, E.; Melik-Nubarov, N. et al. A new class of Drug Carriers: Micelles of poly(oxyethylene)-poly(oxypropylene) Block Copolymers

as Microcontainers for Drug Targeting From the Blood in Brain. *Journal of Controlled Release*, **1992**, 22, 141-157.

(58) Alakhov, V.; Kabanov, A. Block Copolymeric Biotransport Carriers as Versatile Vehicles for Drug Delivery. *Expert Opinion on Investigational Drugs*, **1998**, 7, 1453-1473.

(59) Venne, A.; Li, S.; Mandeville, R.; Kabanov, A.; Alakhov, V. Hypersensitizing Effect of Pluronic L61 on Cytotoxic Activity, Transport, and Subcellular Distribution of Doxorubicin in Multiple Drug-Resistant Cells. *Cancer Research*, **1996**, 56, 3626-3629.

(60) Kuwano, M.; Toh, S.; Uchiumi, T.; Takano, H.; Kohno, K.; Wada, M. Multi-Drug Resistant-Associated Protein Subfamily Transporters and Drug Resistance. *Anticancer Drug Design*, **1999**, 6, 123-131.

(61) Breuninger, L.; Paul, S.; Gaughan, K. et al. Expression of Multidrug Resistance-Associated Protein in NIH/3T3 Cells Confers Multidrug Resistance Associated with Increased Drug Efflux and Altered Intracellular Drug Distribution. *Cancer Research*, **1995**, 55, 5342-5347.

(62) Nooter, K.; Stoter, G. Molecular Mechanims of Multidrug Resistance in Cancer Chemotherapy. *Pathology, Research, and Practice*, **1996**, 192, 768-780.

(63) Cleary, I.; Doherty, G.; Moran, E.; Clynes, M. The Multidrug Resistance Human Lung Tumor Cell Line, DLKP-A10, Expresses Novel Drug Accumulation and Sequestration Systems. *Biochemistry and Pharmacology*, **1997**, 53, 1493-1502.

(64) Shapiro, A.; Fox, K.; Lee, P.; Yang, Y.; Ling, V. Functional Intracellular P-glycoprotein. *International Journal of Cancer*, **1998**, 76, 857-864.

(65) Altan, N.; Chen, Y.; Schindler, M.; Simon, S. Defective Acidification in Human Breast Tumor Cells and Implications for Chemotherapy. *Journal of Experimental Medicine*, **1998**, 187, 1583-1598.

(66) Batrakova, E.; Li, S.; Alakhov, V.; Kabanov, A. Selective Energy Depletion and Sensitization of Multiple Drug Resistant Cancer Cells by Pluronic Block Copolymers. *Polymer Preprints*, **2000**, 41, 1639-1640.

(67) Batrakova, E.; Li, S.; Elmquist, W.; Miller, D.; Alakhov, V.; Kabanov, A. Mechanism of sensitization of MDR Cancer Cells by Pluronic Block Copolymers: Selective Energy Depletion. *British Journal of Cancer*, **2001**, 85, 1987-1997.

(68) Lowe, A.; McCormick, C. Reversible Addition-Fragmentation Chain Transfer (RAFT) Polymerization and the Synthesis of Water-soluble Copolymers Under Homogeneous Conditions in Organic and Aqueous Media. *Progress in Polymer Science*, **2007**, 32, 283-351.

(69) Chiefari, J.; Chong, Y.; Ercole, F.; Krstina, J.; Jeffery, J.; Le TPT, et al. Living Free-radical Polymerization by Reversible Addition-Fragmentation Chain Transfer: The RAFT Process. *Macromolecules*, **1998**, 31, 5559-5562.

(70) Mayadunne, R.; Rizzardo, E.; Chiefari, J.; Chong, Y.; Moad, G.; Thang, S. Living Radical Polymerization with Reversible Addition-Fragmentation Chain Transfer (RAFT Polymerization) Using Dithiocarbamates as Chain Transfer Agents. *Macromolecules*, **1999**, 32, 6977-6980.

(71) Chong, Y.; Le, TPT; Moad, G.; Rizzardo, E.; Thang, S. A More Versatile Route to Block Copolymers and Other Polymers of Complex Architecture by Living

Radical Polymerization: The RAFT Process. *Macromolecules*, **1999**, 32, 2071-2074.

(72) Favier, A.; Charreyre, M-T. Experiemtal Requirements for an Efficient Control of free-radical polymerization via the Reversible Addition-Fragmentation Chain Transfer (RAFT) Process. *Macromolecule Rapid Communications*, **2006**, 27, 653-692.

(73) Corpart, P.; Charmot, D.; Biadatti, T.; Zard, S.; Michelet, D. Inventors. Method for Block Polymer Synthesis by Controlled Radical Polymerization. WO 98/58974. **1998**.

(74) Chong, Y.; Krstina, J.; Le, TPT; Moad, G.; Postma, A.; Rizzardo, E.; et al. Thiocarbonylthio Compounds [S=C(Ph)S-R] in Free Radical Polymerization with Reversible Addition-Fragmentation Chain Transfer (RAFT Polymerization). Role of the Free Radical Leaving Group (R). *Macromolecules*, **2003**, 36, 2256-2272.

(75) Chiefari, J.; Mayadunne, RTA; Moad, C.; Moad, G.; Rizzardo, E.; Postma, A.; et al. Thiocarbonylthio compounds (S=C(Z)S-R) in Free Radical Polymerization with Reversible Addition-Fragmentation Chain Transfer (RAFT Polymerization). Effect of the Activating Group Z. *Macromolecules*, **2003**, 36, 2273-2283.

(76) Donovan, M.; Lowe, A.; Sumerlin, B.; McCormick, C. RAFT polymerization of n,n-dimethylacrylamide Utilizing Novel Chain Transfer Agents for High Reinitiation Efficiency and Structural Control. *Macromolecules*, **2002**, 36, 4123-4132.

(77) Rizzardo, E.; Chiefari, J.; Mayadunne, RTA; Moad, G.; Thang, S. Synthesis of Defined Polymers by Reversible Addition-Fragmentation Chain Transfer : The RAFT Process. In: Matyjaszewski, K, (Ed). Controlled/Living Radical Polymerization: Progress in ATRP, NMP, and RAFT. Wahington, DC: American Chemical Society, **2000**, pp 278-296.

(78) Matyjaszewski, K.; Xia, J. Atom Transfer Radical Polymerization. *Chemistry Review*, **2001**, 101, 2921-2990.

(79) Davis, K.; Matyjaszewski, K. Atom Transfer Radical Polymerization of *tert*-Butyl Acrylate and Preparation of Block Copolymers. *Macromolecules*, **2000**, 33, 4039-4047.

(80) Scott, N. D.; Walker, J. F.; Hansley, V. L. Sodium Naphthalene. I. A New Method for the Preparation of Addition Compounds of Alkali Metals and Polycyclic Aromatic Hydrocarbons. *Journal of the American Chemical Society*, **1936**, 58, 2442-2444.

(81) Hao, J,; Yaun, G.; He, W.; Cheng, H,; Han, C.; Wu, C. Interchain Hydrogen-Bonding-Induced Association of Poly(acrylic acid)-graft-poly(ethylene oxide) in Water. Macromolecules, **2010**, 43, 2002-2008

(82) Atkins et al. Preparing Polyether Polyols with DMC Catalysts. Patent No.: US 7,423,112 B2, **2008**.

(83) Monack, D.; Bouley, D.; Falkow, S. Salmonella typhimurium Persists within Macrophages in the Mesenteric Lymph Nodes of Chronically Infected Nramp1 +/+ Mice can be Reactivated By IFN-gamma Neutralization. *Journal of Experimental Medicine*, **2004**, 199, 231-241.

(84) Galdiero, F.; Carratelli, C.; Nuzzo, I.; Bentivoglio, C.; De Martino, L.; Folgore, A; Galdiero M. Enhancd Cellular Response in Mice Treated with a Brucella

Antigen-Liposome Mixture. *FEMS Immunological Medicine and Microbiology*, **1995**, 10, 235-243.

(85) Gaspar, M.; Cruz, A.; Penha, A.; Reymao, J.; Sousa, A.; Eleuterio, C.; Domingues, S.; Fraga, A.; Filho, A.; Cruz, M.; Pedrosa, J. Rifabutin Encapsulated in Liposomes Exhibits Increased Therapeutic Activity in a Model of Disseminated Turberculosis. *International Journal of Antimicrobiological Agents*, **2008**, 31, 37-45.

(86) Pandey, R.; Khuller, G. Nanoparticle-based Oral Drug Delivery System for an Injectable Antibiotic-Streptomycin. Evaluation in a Murine Turberculosis Model. *Chemotherapy*, **2007**, 53, 437-441.

(87) Cordeiro, C.; Wiseman, D.; Lutwyche, P.; Uh, M.; Evans, J.; Finlay, B.; Webb, M. Antibacterial Efficacy of Gentamicin Encapsulated in pH-sensitive Liposomes Against an In Vivo Salmonella Enterica Serovar Typhimurium Intracellular Infection Model. *Antimicrobial Agents and Chemotherapy*, **2000**, 44, 533-539.

(88) Liu, Y.; Prud'homme, R. Mixing in a Multi-Inlet Vortex Mixer (MIVM) for Flash Nano-Precipiation. *Chemical Engineering Science,* **2008**, 63, 2829-2842.

(89) Ranjan, A.; Saleem, M.; Jain, J.; Sriranganathan, N.; Riffle, J.S.; Kasimanickam, R. Drug Delivery Using Novel Nanoplexes Against a Salmonella Mouse Infection Model. *Journal of Nanoparticle Research*, **2009**.

(90) Kaale, E.; Govaerts, C.; Hoogmartens, J.; Schepdael, A. Mass Spectrometric Study to Characterize Thioisoindole Derivatives of Aminoglycoside Antibiotics. *Rapid Communications in Mass Spectrometry*, **2005**, 19, 2918-2922.

(91) Stobaugh, J.; Repta, A.; Sternson, L.; Garren, K. *Analytical Biochemistry*, **1983**, 135, 495.

(92) Simons, S, Jr.; Johnson, D. *Analytical Biochemistry*, **1977**, 82, 250

(93) Simons, S, Jr.; Johnson, D. *Analytical Biochemistry*, **1978**, 90, 705

(94) Nakamura H.; Matsumoto A.; Tamura Z. *Analytical Letters*, **1982**, 15, 1393.